sustainability

MDPI

Article

Sustainable Groundwater Management in the Coastal Aquifer of the Témara Plain, Morocco: A GIS-Based Hydrochemical and Pollution Risk Assessment

Abdessamia El Alaoui [1], Imane Haidara [2], Nawal Bouya [3], Bennacer Moussaid [1], Khadeijah Yahya Faqeih [4], Somayah Moshrif Alamri [4], Eman Rafi Alamery [4], Afaf Rafi AlAmri [5], Youness Moussaid [6] and Mohamed Ait Haddou [6,*]

[1] Interdisciplinary Laboratory of Fundamental and Applied Sciences, Ecole Normale Supérieure, Hassan II University, Casablanca 50069, Morocco
[2] Department of Geology, Faculty of Sciences Ben M'sik, Hassan II University, Casablanca 20000, Morocco
[3] Department of Geology, Faculty of Sciences, Moulay Ismail University, Meknes 50050, Morocco
[4] Department of Geography and Environmental Sustainability, College of Humanities and Social Sciences, Princess Nourah bint Abdulrahman University, P.O. BOX 84428, Riyadh 11671, Saudi Arabia
[5] Department of Geography, College of Humanities and Social Sciences, King Saud University, Riyadh 11451, Saudi Arabia
[6] Department of Earth Sciences, Faculty of Sciences, Ibn Zohr University, Agadir 80000, Morocco
* Correspondence: mohamed.aithaddou@uit.ac.ma

Abstract: Morocco's Témara Plain relies heavily on its aquifer system as a critical resource for drinking water, irrigation, and industrial activities. However, this essential groundwater reserve is increasingly threatened by over-extraction, seawater intrusion, and complex hydrogeochemical processes driven by the region's geological characteristics and anthropogenic pressures. This study aims to assess groundwater quality and its vulnerability to pollution risks and map the spatial distribution of key hydrochemical processes through an integrated approach combining Geographic Information System (GIS) techniques and multivariate statistical analysis, as well as applying the DRASTIC model to evaluate water vulnerability. A total of fifty-eight groundwater samples were collected across the plain and analyzed for major ions to identify dominant hydrochemical facies. Spatial interpolation using Inverse Distance Weighting (IDW) within GIS revealed distinct patterns of sodium chloride (Na-Cl) facies near the coastal areas with chloride concentrations exceeding the World Health Organization (WHO) drinking water guideline of 250 mg/L—indicative of seawater intrusion. In addition to marine intrusion, agricultural pollution constitutes a major diffuse pressure across the aquifer. Shallow groundwater zones in agricultural areas show heightened vulnerability to salinization and nitrate contamination, with nitrate concentrations reaching up to 152.3 mg/L, far surpassing the WHO limit of 45 mg/L. Furthermore, other anthropogenic pollution sources—such as wastewater discharges from septic tanks in peri-urban zones lacking proper sanitation infrastructure and potential leachate infiltration from informal waste disposal sites—intensify stress on the aquifer. Principal Component Analysis (PCA) identified three key factors influencing groundwater quality: natural mineralization due to carbonate rock dissolution, agricultural inputs, and salinization driven by seawater intrusion. Additionally, The DRASTIC model was used within the GIS environment to create a vulnerability map based on seven key parameters. The map revealed that low-lying coastal areas are most vulnerable to contamination.

Keywords: groundwater; hydrochemistry; GIS; multivariate statistics; DRASTIC; nitrate contamination; vulnerability; seawater intrusion; agricultural practices

Academic Editor: Yong Xiao

Received: 10 April 2025
Revised: 21 May 2025
Accepted: 27 May 2025
Published: 11 June 2025

Citation: El Alaoui, A.; Haidara, I.; Bouya, N.; Moussaid, B.; Faqeih, K.Y.; Alamri, S.M.; Alamery, E.R.; AlAmri, A.R.; Moussaid, Y.; Ait Haddou, M. Sustainable Groundwater Management in the Coastal Aquifer of the Témara Plain, Morocco: A GIS-Based Hydrochemical and Pollution Risk Assessment. *Sustainability* **2025**, *17*, 5392. https://doi.org/10.3390/su17125392

1. Introduction

Water resources are under unprecedented pressure in the 21st century, driven by the escalating demands of a growing global population, rapid urbanization, and intensified agriculture. This strain is particularly acute for freshwater resources, impacting both surface water and groundwater systems [1–3]. Groundwater, often a more reliable and higher-quality source than surface water [4–6], plays a critical role in mitigating the effects of climate variability, especially in arid and semi-arid regions where surface water availability is frequently limited [7,8]. However, these vital subsurface reserves are increasingly vulnerable to degradation caused by a complex interplay of natural and human-induced pressures, including over-extraction, contamination, and the cascading effects of climate change. The Mediterranean region, already a hotspot for water scarcity [9,10], is emblematic of these challenges and provides a critical context for understanding regional groundwater vulnerabilities. Coastal aquifers, like those along Morocco's Atlantic coastline, are particularly susceptible to these combined pressures. The Témara Plain aquifer exemplifies this vulnerability, mirroring challenges observed in other Mediterranean coastal systems [11–14]. Such as the Agadir aquifer in Morocco [15,16] and coastal aquifers in Spain [17,18], which face seawater intrusion, agricultural contamination, and urban effluent pressures. While the specific drivers and hydrogeological contexts vary, these regions share the common challenge of balancing growing water demands with the need to protect vulnerable coastal groundwater resources.

The convergence of rising water demand, seawater intrusion driven by over-extraction and sea-level rise, and diffuse pollution from agricultural and urban activities pose significant threats to the long-term sustainability of these critical groundwater systems [19,20]. Furthermore, climate change impacts, including shifting precipitation patterns, increased evapotranspiration, and more frequent and intense droughts, exacerbate these challenges by reducing groundwater recharge and intensifying salinization [21,22]. Morocco, a nation grappling with significant water stress, relies heavily on groundwater to meet the demands of its population, agriculture, and industry [23,24]. The Témara Plain, situated along Morocco's Atlantic coast, epitomizes this dependence. Its aquifer system supplies water for over 1.2 million people and irrigates approximately 15,000 hectares of farmland, making it an essential resource for the region's social and economic well-being [25]. However, this vital aquifer is increasingly imperiled. Over-extraction, exceeding natural recharge by more than 20% annually, is contributing to declining water tables and elevated risk of seawater intrusion. Concurrently, intensive fertilizers use of fertilizers in agriculture, combined with rapid urbanization and industrial expansion, contribute to diffuse pollution, jeopardizing the quality and safety of this essential water source. The hydrogeological setting of Témara Plain, characterized by a complex mosaic of carbonate rocks, marl, and alluvial deposits [26,27], further complicates groundwater resource management in this area. This geological heterogeneity influences both the flow patterns and groundwater chemical composition, resulting in spatially variable salinity and mineral content. Understanding the intricate interactions between the aquifer's geological framework, natural hydrogeochemical processes, and superimposed anthropogenic pressures is paramount for effective and sustainable groundwater management in the region. While previous studies in the Témara Plain and analogous coastal aquifers across the Mediterranean have shed light on specific aspects of groundwater systems, such as salinization [28–31], recharge dynamics, or individual contaminant pathways, a comprehensive understanding of the interplay between these multiple stressors remains elusive. These works, often constrained by the limited number of sampled points and their spatial distribution, have lacked the required resolution-systematic distribution of sampled points along the studied area to effectively characterize contamination plumes or pinpoint vulnerable areas within the

Témara Plain aquifer. In addition to these well-known pressures, recent scientific findings emphasize the importance of integrating dynamic geophysical factors—particularly seismic activity—into vulnerability assessments of coastal aquifers. Seismic events can alter groundwater pressure and aquifer permeability, potentially accelerating inland seawater intrusion and modifying hydrochemical gradients in complex ways [32].

The concept of vulnerability mapping constitutes an essential component of groundwater contamination risk assessment. These maps provide a spatial representation of aquifers' sensitivity to potential pollution based on various environmental, hydrogeological, and anthropogenic factors. The aim is not to measure a current state of pollution but rather to estimate a hydrogeological system's capacity to transmit pollutants from the surface to the water table. The design of these maps is based on various methodological approaches, grouped into three main categories: index-based models such as DRASTIC, statistical approaches, and deterministic or physical–mathematical models [33]. The integration of these methods into a GIS (Geographic Information System) environment allows the production of synthetic maps with high decision-making value.

As part of the study conducted in the Témara Plain, advanced analysis tools were employed prior to applying the DRASTIC model. A spatial interpolation using the Inverse Distance Weighting (IDW) method with a 500 m resolution was carried out to map salinity and nitrate gradients. In parallel, a Principal Component Analysis (PCA) was performed to identify covariant patterns among hydrochemical parameters [34,35]. These preparatory steps help better characterize the natural and anthropogenic controlling factors influencing groundwater quality and provide a robust foundation for constructing the vulnerability map. Vulnerability maps rely on key parameters such as depth to the water table, effective recharge, aquifer material type, soil type, topographic slope, unsaturated zone, and hydraulic conductivity. Each parameter is assigned a rating and a weight reflecting its relative influence on pollution risk, enabling the calculation of a composite index and the production of a thematic map [33].

These cartographic tools are fundamental for guiding sustainable water management policies, defining protection perimeters, prioritizing monitoring zones, and informing land-use planning. However, despite methodological advances, the design of vulnerability maps still faces major challenges, particularly regarding the integration of complex interactions between natural processes and anthropogenic pressures and the accurate representation of hydrochemical dynamics in heterogeneous environments.

This study integrates high-resolution GIS mapping and PCA to (1) delineate hydrochemical facies, (2) quantify anthropogenic vs. natural influences, and (3) identify priority zones for management. This work provides the first spatially explicit assessment of combined seawater intrusion and agricultural pollution in the Témara Plain, leveraging a dense sampling network (58 wells) and advanced interpolation methods. This study addresses this knowledge gap by conducting a comprehensive assessment of groundwater quality in the Témara Plain. By integrating hydrochemical analyses, high-resolution spatial mapping using ArcGIS v10.8 software, and multivariate statistical techniques, we address the following key research questions:

- What are the dominant hydrochemical facies in the Témara Plain aquifer and their spatial distribution?
- What are the controlling factors, natural and anthropogenic, of the groundwater chemistry in the studied region?
- What is the vulnerability of the Témara Plain aquifer to seawater intrusion and agricultural contamination?

By exploring these questions, this research aims to provide a comprehensive assessment of the factors influencing groundwater quality in the Témara Plain, informing

sustainable water resource management strategies within the region and offering valuable insights applicable to similar coastal aquifers worldwide. Furthermore, it contributes directly to achieving SDG 6 and SDG 13 [36–38] within the framework of Morocco's national water strategies.

2. Study Area

2.1. Geological Setting

The Témara Plain (Figure 1), located along Morocco's Atlantic coast, features a complex geology of Quaternary and Tertiary formations. Surface deposits of sands, gravels, and clays (alluvial, coastal dune, and fluvial) create high-permeability zones facilitating groundwater recharge in the underlying Miocene and Pliocene marine limestones, marls, and clays [39].

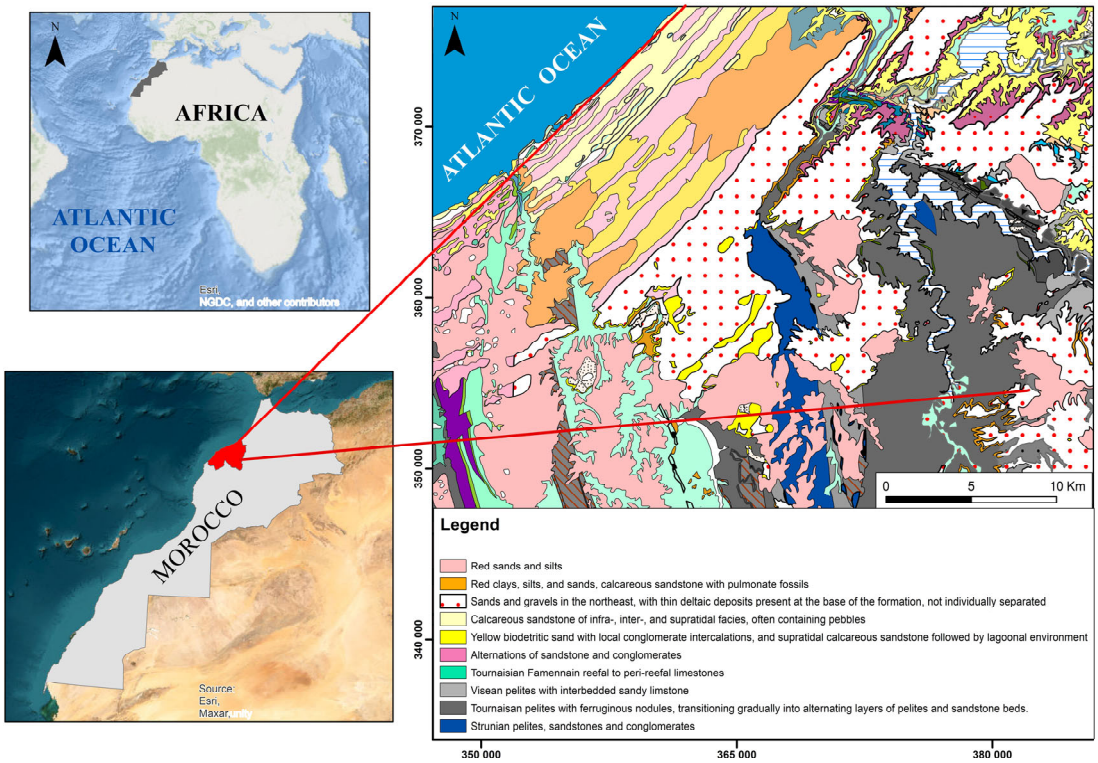

Figure 1. Study area location within the geological context of the Témara Plain, showing major faults and lithological units (modified from [40]).

Significantly influence groundwater chemistry through mineral dissolution and cation exchange processes. Carbonate-rich units increase groundwater hardness, while clays reduce permeability and form confined aquifers regulating groundwater flow [7,41]. Fault zones can act as preferential flow conduits or barriers, impacting recharge and lateral movement. This structural complexity creates spatially heterogeneous groundwater quality with varying salinity and mineral composition. Paleozoic basement rocks (shales and sandstones) exposed inland further influence groundwater chemistry. The region's geomorphology—gentle undulations, coastal plains, stabilized dunes, and bioclastic limestone ridges—reflects marine erosion, sedimentation, and tectonic uplift [42], leading to a complex hydrogeological framework. Secondary porosity, particularly in calcarenites and karstified limestones, enhances hydraulic conductivity, increasing susceptibility to contamination and marine intrusion. The Témara region's Mediterranean climate, moderated by the Atlantic, features hot, dry summers and mild, wet winters. Rainfall (300–500 mm annually) is concentrated between November and March. Oceanic winds influence both evaporation

and recharge. However, increasingly frequent droughts, exacerbated by climate change [43], threaten groundwater sustainability.

2.2. Land Use

Land use in the Témara region has undergone significant changes linked to rapid urban expansion and agricultural intensification (Figure 2). The growing population and rising water demand are stressing groundwater resources. Industrial and residential areas contribute to pollution through wastewater and runoff, introducing heavy metals and organic contaminants, which further burden the aquifer. Intensive agriculture, especially in peri-urban areas like Sidi Yahia and Ain Attig, relies on nitrogen-based fertilizers, leading to elevated nitrate levels in groundwater.

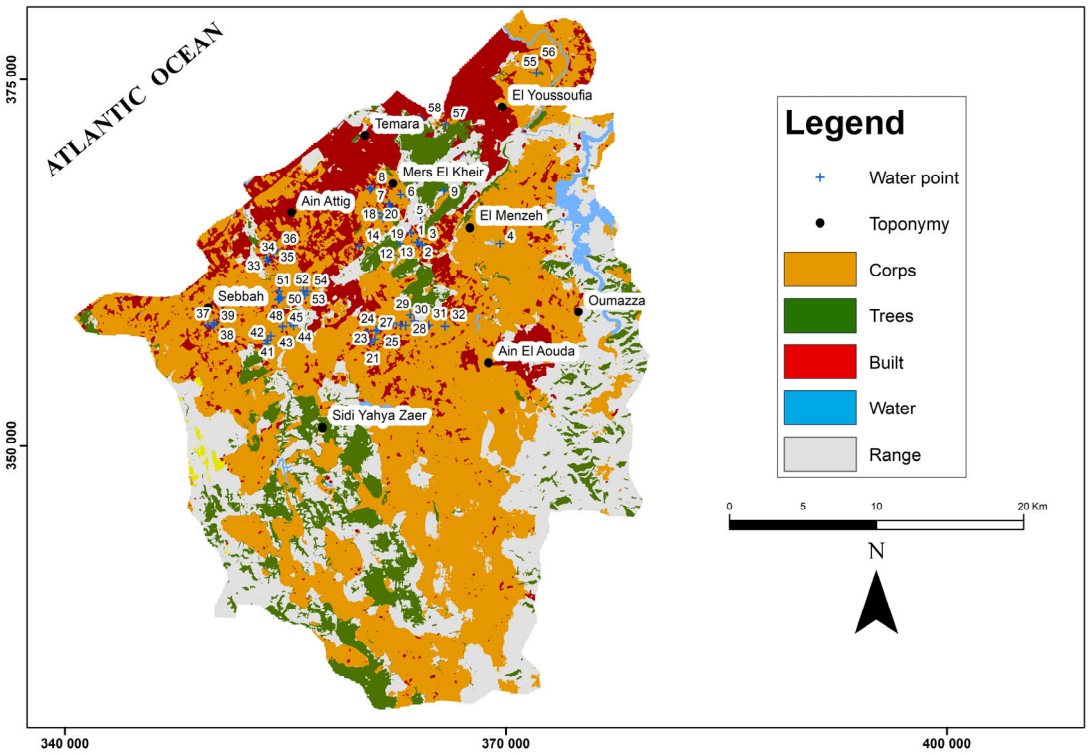

Figure 2. Urban expansion, agricultural intensification, and groundwater sampling locations in the Témara region (source: ArcGIS Living Atlas Land Cover Explorer, 2024).

This contamination of the area compromises drinking water supplies and ecosystems. The overuse of pesticides and herbicides further degrades water quality by introducing persistent pollutants. Deforestation and land degradation disrupt natural infiltration, increasing surface runoff and reducing groundwater recharge. Excessive groundwater extraction along the coast triggers seawater intrusion [20], threatening freshwater availability. The resulting salinization compromises water quality and poses a long-term risk to agricultural productivity and food security. Sustainable land management is, therefore, critical. Mitigation strategies such as drip irrigation, terracing, and other controlled irrigation and soil conservation techniques, combined with the cultivation of water-efficient crops and soil conservation techniques, can reduce these impacts. Integrated water resource management, encompassing regulated extraction and artificial recharge, is essential for maintaining the aquifer's long-term health.

3. Materials and Methods

3.1. Sampling and Analytical Methods

Fifty-eight groundwater samples were collected across the Témara Plain to assess water quality based on various physicochemical parameters (Table 1). The sampling strategy was carefully designed to ensure balanced spatial coverage across the diverse environments of the Témara Plain, including agricultural, urban, and coastal areas. Selection criteria incorporated both land-use intensity and hydrogeological vulnerability to guarantee a statistically robust representation of the region. To achieve comprehensive coverage, sampling was carried out at nearly all accessible and available locations, following a systematic and representative distribution pattern (Figure 2). Electrical conductivity (EC) and temperature were measured on-site using a calibrated EUTECH INSTRUMENTS Conductivity Meter, with electrodes rinsed in distilled water between measurements [44]. pH was determined using a Palin pH meter calibrated with standard buffer solutions before each use. Laboratory analyses included the quantification of major ions and other key parameters. Chloride (Cl^-) concentrations were determined by argentometric titration with a silver nitrate solution using potassium chromate as an indicator. Sulfate (SO_4^{2-}) and nitrate (NO_3^-) concentrations were determined spectrophotometrically (HACH LANGE).

Table 1. Descriptive statistics of groundwater analytical results from the Témara Plain.

Chemical Parameter	Units	Minimum	Maximum	Mean	WHO Drinking Water Guidelines (2011)
pH	-	6.69	7.89	7.27	6.5–8.5
E.C	(µS/cm)	2741	4817	3877.31	500–1000
Ca^{2+}	(mg/L)	9.14	123.4	41.30	200
Mg^{2+}	(mg/L)	13.9	56.9	34.62	50
Na^+	(mg/L)	4.32	360	130.06	200
K^+	(mg/L)	1.55	98.1	26.82	200
HCO_3^-	(mg/L)	87	594	359.15	500
Cl^-	(mg/L)	68.2	721	349.60	250
SO_4^{2-}	(mg/L)	17.6	94.5	40.93	250
NO_3^-	(mg/L)	0.29	152.3	50.22	45

Bicarbonate (HCO_3^-) was measured by titration with sulfuric acid following the standard method for alkalinity determination, and calcium (Ca^{2+}) was measured by complexometric titration with EDTA (ethylenediaminetetraacetic acid). Sodium (Na^+) and potassium (K^+) concentrations were analyzed via flame spectrophotometry HACH® Data processing and visualization were performed using several software tools. ArcMap 10.8 was used to define the study area and map the spatial distribution of chemical elements. Piper and Wilcox diagrams were generated using Diagrammes v8.44 software. Descriptive statistics and multivariate analyses were performed using XLSTAT 2025 v26.4.1.0 Addinsoft. Water quality standards were based on the WHO "Guidelines for Drinking-water Quality: Fourth Edition" [45].

3.2. Study of Hydrochemical Facies

Hydrochemical facies and irrigation suitability were assessed using Piper and Wilcox diagrams v8.44. These diagrams were generated using Aquachem software (v12.0) to assess hydrochemical facies and irrigation suitability [19]. The Piper diagram visualizes the relative proportions of major cations (Ca^{2+}, Mg^{2+}, Na^+, K^+) and anions (HCO_3^-, SO_4^{2-}, Cl^-) to identify hydrochemical water types and infer geochemical processes [25]. The Wilcox diagram evaluates water quality for irrigation based on salinity and sodium

adsorption ratio (SAR) to determine potential impacts on soil structure and crop health [46]. The software also enabled correlation analysis between chemical parameters, aiding in the identification of contamination sources and assessment of anthropogenic impacts [47–50].

3.3. Spatial Distribution Analysis

The spatial distribution of hydrochemical parameters across the Témara region was assessed through Inverse Distance Weighting (IDW) interpolation [34,35]. IDW was selected for its simplicity and robustness, making it particularly suitable for the irregular distribution of sampling points and the heterogeneous nature of the groundwater chemistry in the study area [51–54]. Among other considered interpolation methods (kriging and splines), each one presented limitation. Kriging, while accurate, requires complex spatial modeling and can introduce uncertainties with limited datasets, as was the case in this study [55]. Splines can generate unrealistic values when applied to highly variable hydrochemical data [34]. The IDW method assigns a weight (w_i) to each measurement point inversely proportional to the distance (d_i) raised to a power parameter (p):

$$w_i = \frac{1}{\left\{d_i^p\right\}} \tag{1}$$

An optimal p-value of 0.052 was determined through iterative testing [55,56] to optimize results and minimize potential bias.

The estimated value at a point x is calculated as the weighted average of observed values (V_i):

$$V(x) = \frac{\sum_{i=1}^{n} w_i \cdot V_i}{\sum_{i=1}^{n} w_i} \tag{2}$$

To evaluate the accuracy of IDW relative to kriging, we performed leave-one-out cross-validation (LOOCV) and computed two key performance indicators.

The coefficient of determination ($\boldsymbol{R^2}$), which indicates how well the interpolation model explains the observed variability, is defined as follows:

$$\boldsymbol{R^2} = \mathbf{1} - \frac{\sum_{i=1}^{n}(\boldsymbol{O_i} - \boldsymbol{P_i})^2}{\sum_{i=1}^{n}(\boldsymbol{O_i} - \overline{\boldsymbol{O}})^2} \tag{3}$$

where $\boldsymbol{O_i}$ is the observed value, $\boldsymbol{P_i}$ is the predicted value, and $\overline{\boldsymbol{O}}$ is the mean of observed values. An $\boldsymbol{R^2}$ value approaching 1 indicates high predictive accuracy.

The Root Mean Square Error (RMSE) quantifies the average deviation between observed and predicted values:

$$\text{RMSE} = \sqrt{\frac{\mathbf{1}}{\boldsymbol{n}}\sum_{i=1}^{n}(\boldsymbol{O_i} - \boldsymbol{P_i})^2} \tag{4}$$

Lower RMSE values indicate more precise estimations.

Both $\boldsymbol{R^2}$ and RMSE were calculated for IDW and kriging, with the results detailed in Table 2. In this study, IDW achieved $\boldsymbol{R^2}$ values ranging from 0.75 to 0.87 and yielded lower RMSE values than kriging for most parameters (e.g., NO_3^-, EC, Cl^-), confirming the effectiveness of this method in the specific hydrogeological context of the study area.

Table 2. Comparison of interpolation performance between IDW and kriging methods for hadrochemical parameters.

Parameter	Method	R^2 (Cross-Validation)	RMSE
EC	IDW	0.87	310
EC	Kriging	0.84	340
NO_3^-	IDW	0.79	18.4
NO_3^-	Kriging	0.77	19.6
Cl^-	IDW	0.75	27.1
Cl^-	Kriging	0.81	19.2

3.4. Principal Component Analysis (PCA) of Hydrochemical Data

Principal component analysis (PCA) was applied to the hydrochemical dataset (Table 3) to reduce dimensionality and identify key factors influencing groundwater chemistry. While traditional PCA effectively captured primary variations, integrating machine learning (ML) offers promising enhancements. For example, refs. [57,58] highlight ML's growing role in materials research, spanning characterization to synthesis planning. Combining ML with PCA could improve feature extraction, parameter optimization, and interpretability. Furthermore, ML-based clustering methods, such as combining extreme learning machines with PCA [59] or using self-organizing maps [60], offer complementary analytical approaches. Studies like Goodarzi et al. [61] demonstrate the potential of ML models (CNN, SVM, DT) for groundwater prediction. Integrating ML with PCA represents a promising future direction for enhanced hydrochemical analysis, potentially revealing more nuanced relationships within the data.

3.5. Groundwater Vulnerability Assessment

The DRASTIC model was implemented to integrate multiple hydrogeological and environmental factors, thereby deriving a comprehensive vulnerability index. This integrated approach enabled the generation of a detailed vulnerability map, pinpointing areas within the Témara aquifer most susceptible to contamination [33]. The development of this vulnerability map involved creating thematic raster layers for each of the seven DRASTIC parameters. This layer-overlay technique, a common multi-criteria approach, has been previously employed in environmental assessments [62,63]. The synergistic application of these geospatial techniques for DRASTIC modeling, together with the preceding multivariate statistical analysis for hydrochemical characterization, established a robust framework for the overall groundwater vulnerability assessment. This comprehensive assessment is crucial for informing sustainable water resource management strategies in the Témara region.

The DRASTIC index, formulated as shown in Equation (5), served as the primary tool for evaluating aquifer susceptibility to contamination. This index incorporates seven key hydrogeological parameters originally defined by Aller et al. [64]: depth to groundwater (D), net recharge (R), aquifer material type (A), soil type (S), topography (T), unsaturated zone impact (I), and hydraulic conductivity (C). For each parameter, distinct classes were established based on local hydrogeological conditions, and each class was subsequently assigned a numerical rating (r) ranging from 1 to 10, where higher ratings signify greater vulnerability.

$$\mathrm{DI} = D_r \times D_w + R_r \times R_w + A_r \times A_w + S_r \times \mathrm{w} + T_r \times T_w + C_r \times C_w \quad (5)$$

The accurate assignment of these parameter ratings necessitates a thorough understanding of the study area's specific geological and hydrogeological context [65].

The resulting DRASTIC index values quantify the degree of groundwater susceptibility to contamination. These values are typically categorized into vulnerability classes, as established by Aller et al. [64]. The final DRASTIC vulnerability index map was produced by integrating the seven hydrogeological parameter layers using the raster calculator tool within ArcGIS software. Consistent with the DRASTIC methodology, each parameter was assigned a specific weight (*w*) reflecting its relative influence on pollution susceptibility. In contrast, the rating (*r*) for each parameter was determined from its corresponding thematic layer based on site-specific conditions. These weights and the rating system are detailed in Table 3.

Table 3. DRASTIC model parameters: assigned rating (r) and weights (w) scales for vulnerability classes [64].

Parameters	Classes	Index (r)	Weight (w)
D	<1.50	10	5
	1.50–4.60	9	
	4.60–9.10	7	
	9.10–15.20	5	
R	0–51	1	4
A	Metamorphic/igneous rock	2–5 (3)	3
	Altered metamorphic/igneous rocks	3–5 (4)	
	Sand and ballast	4–9 (8)	
S	Thin or absent	10	2
	Sand	9	
	Loam	5	
	Clay loam	3	
	Non-aggregated and non-expandable clay	1	
T	<2	10	2
	2–6	9	
	6–12	5	
	12–19	3	
	>18	1	
I	Metamorphic/igneous rock	2–8 (4)	5
	Sand and ballast with significant silt andclay percentage	4–8 (6)	
C	<4.10	1	3
	4.10–12.20	2	

4. Results

Groundwater samples from the 58 wells were analyzed for various physicochemical parameters, and the mean annual values are summarized in Table 4. The first examination of results shows that 15 wells, predominantly located in the northern sector of the Témara Plain, display chloride concentrations exceeding the WHO drinking water standard of 250 mg/L.

Table 4. Mean annual values of physicochemical parameters for groundwater from 58 wells in the Témara Plain.

Wells	pH	EC (µS cm^{-1}) at 25 °C	Ca^{2+} (mg L^{-1})	Mg^{2+} (mg L^{-1})	Na^{+} (mg L^{-1})	K^{+} (mg L^{-1})	HCO_3^{-} (mg L^{-1})	Cl^{-} (mg L^{-1})	SO_4^{2-} (mg L^{-1})	NO_3^{-} (mg L^{-1})
Z1	7.01	2950	19.1	38.4	281.5	4.24	280	614	22.8	8.77
Z2	6.95	2988	47	39.8	194.3	5.12	354	355.8	37.9	17.16
Z3	7.15	2895	18.9	25.1	190.7	5.66	394	398.6	41.5	18.05
Z4	7.53	2741	12.8	30.1	215.9	7.14	469	480	55.6	16.55
Z5	7.59	3250	20.7	36.5	360	21.7	470	590	45.9	0.29
Z6	7.08	3189	16.8	40.6	211	23.9	510	482	37.4	2.55
Z7	6.88	3546	20.11	13.9	189	15.8	388	486	47.9	10.5
Z8	7.89	3015	14.8	19.8	265	17.9	452	510	44.6	5.14
Z9	6.69	3022	15.4	22.8	354	18.2	476	524	27.1	6.88
Z10	7.11	3210	19.1	18.4	248	4.24	482	617	20.2	8.77
Z11	7.4	3340	13.6	24.1	245.3	5.13	423	340	24.6	16.8
Z12	7.88	3250	14.56	17.8	136.8	8.9	500	403	44.8	20.1
Z13	7.88	2978	9.14	24.7	138.9	1.55	409	407	44.8	36.5
Z14	6.91	3215	17.8	14.9	245.3	11.2	416	433	25.9	17.2
Z15	6.94	3088	26.4	15.6	189	29.8	470	698	35.6	25.6
Z16	7.19	3214	24.8	20.7	153.8	35.4	397	655.4	33.7	40.1
Z17	7.3	3102	50.1	25.4	139.8	7.88	433	470	38.6	22.6
Z18	7.55	3076	19.8	35.6	140.1	15.9	400	536	42.8	36.5
Z19	7.19	3491	10.7	30.6	145.6	12.3	453	419	48.6	58.9
Z20	7.2	3150	15.4	33.9	149	15.8	400	549	46.9	51.8
Z21	6.88	4112	15.7	24.6	6.7	13.2	594	90.5	23.4	15.5
Z22	7.06	4013	12.3	21.7	5.44	17.6	546	88.4	36.7	23.9
Z23	7.4	4235	22.1	34.6	7.55	12.9	501	117	33.8	34.6
Z24	7.63	4002	18.9	29.1	8.26	16.9	546	96.3	40.8	26.4
Z25	7.8	4250	24.9	35	9.4	20	492	120	40	36
Z26	7.56	4310	22.7	30.7	8.55	14.6	479	115.4	37.6	29.8
Z27	7.05	4066	20.1	31.4	8.15	9.24	503	107	34.6	25.9
Z28	6.84	3954	17.9	34	4.6	13.8	574	109	32.6	19.6
Z29	7.09	4008	24.3	34.2	8.04	15.7	544	106	37.6	31.7
Z30	7.14	4090	19.6	18.4	11.8	16.4	498	96.8	37.8	32.4
Z31	6.94	4077	25.6	34.7	12.4	18	415	96.4	30.6	31.8
Z32	7.6	4255	21.7	34.9	9.6	16.7	433	118	26.8	35.2
Z33	7.13	4211	45.6	35.6	131.8	19.2	160	112	23.7	90.7
Z34	7.44	4356	70.1	46.5	118	36.8	180	544	29.7	74.3
Z35	7.18	4076	76.4	40.1	236.7	44.8	244	526	18.6	84.3
Z36	7.71	4263	70.2	49.3	186.4	36.9	213	648	55.6	112.5
Z37	6.98	4056	72.6	56.9	141.2	14.3	109	315	44.3	114.6
Z38	7.4	4122	70.4	51.2	116.4	45.3	173	681	31.6	132.6
Z39	7.44	4256	80.1	42.1	146	32.5	188	316	55.6	96.8
Z40	7.41	4521	65.8	49.9	156.7	29.3	326	278	27.5	88.6
Z41	7.8	4460	69.8	48.6	162.1	41.7	318	290	31.8	90.4
Z42	7.45	4311	66.9	45.7	265.8	51.2	379	315	17.6	91.4
Z43	7.84	4250	68.9	50.1	160.1	49.6	403	327	23.8	98.5
Z44	6.98	4002	64.1	46.7	41.2	39.8	369	279	19.7	99.3
Z45	7.12	4611	65.1	44.1	223	22.3	378	460	25.4	152.3
Z46	7.32	4325	76.5	39.7	246	77.8	400	655	36.4	123
Z47	6.98	4466	86.4	49.8	287	56.9	398	721	32.7	106
Z48	7.5	4817	102	46.2	148	69.5	367	708	44.9	98.5
Z49	7.39	4435	90.4	50.7	190.4	18.9	382	685	22.8	84.6
Z50	7.26	4274	77.8	47.9	188.6	86.9	309	415	37.1	99.4
Z51	7.24	4109	123.4	51.2	211.5	88.7	412	436	41.8	89.7
Z52	7.17	4026	84.5	55.2	194.2	98.1	419	386	39.1	87.6
Z53	7.02	3987	98.6	52.3	123.4	76	377	496	45.6	97.1
Z54	7.46	4386	94.5	47.9	166.5	74.9	346	401	54.6	102.5
Z55	6.88	4022	14.6	17.4	4.65	11.4	87	68.2	70.4	7.54
Z56	7.12	3956	18.6	22.1	4.32	10.4	96	115	84.6	6.45
Z57	7.21	4076	18.4	20.4	4.69	14.2	106	76.9	74.1	4.56
Z58	7.13	4123	20.1	23.4	5.63	14.7	115	125.4	94.5	9.64

4.1. Hydrochemical Facies

The diagram (Figure 3) illustrates the distribution of major ions in groundwater across various communes. Groundwater samples from Ain Attig, Sidi Yahia, El Menzah, and Mers El Khir predominantly exhibit sodium-chloride or sodium-sulfate facies. This composition likely reflects evaporite minerals (Na, Cl, bearing minerals) dissolution or the influence of saline water intrusion in areas where these geological formations are present. Conversely, groundwater from Sebbah, El Youssoufia, and certain wells in Sidi Yahia is

mainly characterized by calcium-chloride and magnesium-sulfate types. This composition suggests water–rock interactions with clay and marl formations, which can release calcium and magnesium ions during weathering processes. These hydrochemical variations reflect the complex interplay of controlling factors of groundwater chemistry, including water–rock interactions, potential saline water intrusion, and other geochemical processes.

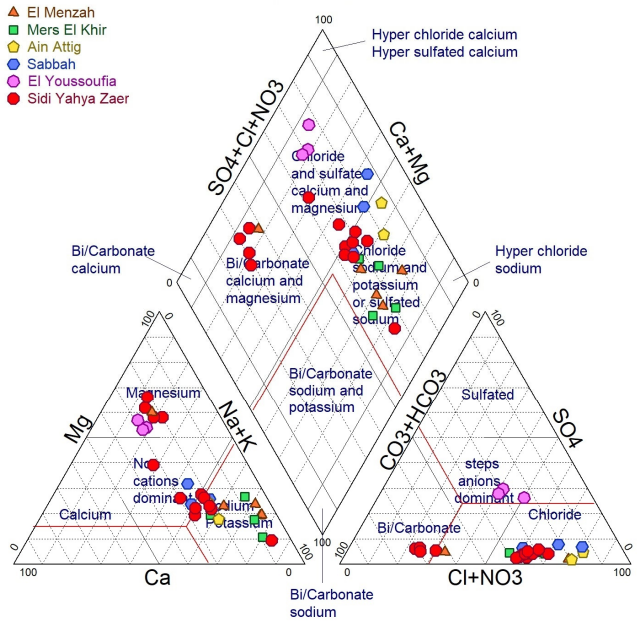

Figure 3. Hydrochemical facies of Témara Plain groundwater represented by a Piper diagram.

Figure 4A shows that groundwater samples from Ain Attig, Sidi Yahia, El Menzah, Sebbah, and Mers El Khir exhibit moderate conductivity values (2000–2250 µS/cm) and low to moderate alkalinity (10–20 mg/L). The moderate conductivity and alkalinity obtained in these areas likely result from the combined effects of mineral dissolution within the aquifer matrix and dilution of recharge water. The Wilcox diagram (Figure 4B) illustrates the sodium hazard classification of groundwater samples. This former reveals that most samples from Sidi Yahia, El Youssoufia, and Sebbah clusters are in the "good to excellent" range for irrigation water quality, indicating low sodium hazard. Whereas Mers El Khir and El Menzah samples are rated as "acceptable", groundwater from Ain Attig is classified as "poor" due to high sodium content. The high sodium concentrations in Ain Attig may be related to agricultural activities, dissolution of specific minerals, and seawater intrusion, consistent with the elevated chloride and sulfate concentrations (Table 4). Further investigations are required to quantify contamination sources and their relative contributions. Previous studies have shown that agricultural runoff, particularly from fertilizer application, can contribute to increased nitrate and sulfate concentrations in groundwater [39]. The geological formations in the area may further modulate groundwater chemistry.

The Piper and Wilcox diagrams provide valuable insights into groundwater chemistry and its suitability for various uses, particularly irrigation. The Piper diagram (Figure 3) illustrates the relative concentrations of major cations and anions, enabling the identification of dominant hydrochemical facies in the Témara Plain. For instance, sodium-chloride (Na-Cl) facies—typically associated with seawater intrusion in coastal aquifers—exhibit elevated sodium and chloride concentrations. Such high salinity makes water unsuitable for irrigation, potentially leading to soil degradation and reduced crop yields. Conversely, calcium-bicarbonate (Ca-HCO_3) facies, commonly found in inland carbonate aquifers, generally indicate good quality water suitable for both potable use and irrigation. The Wilcox diagram (Figure 4B) specifically evaluates irrigation suitability through electrical

conductivity (EC) and sodium adsorption ratio (SAR). High EC values can lead to salt accumulation in agricultural soils and reduced fertility. In the Témara Plain, some groundwater samples exceed moderate EC thresholds, potentially restricting their use for salt-sensitive crops. The integrated interpretation of Piper and Wilcox reveals the complex hydrogeochemical processes governing water chemistry and quality and facilitates science-based water management decisions.

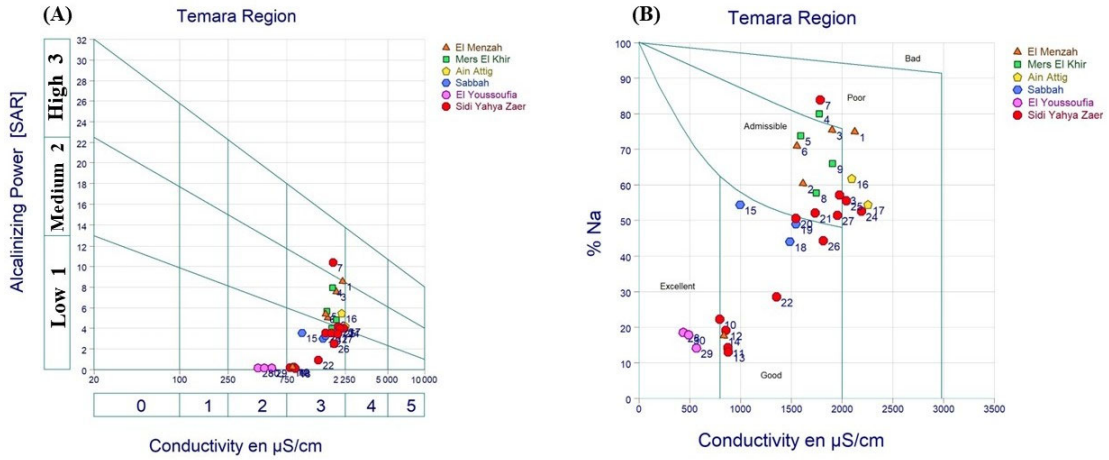

Figure 4. (**A**) Richard's diagram showing the relationship between alkalinity (expressed as HCO_3^- in mg/L) and electrical conductivity (µS/cm); (**B**) Wilcox diagram illustrating sodium hazard versus electrical conductivity (µS/cm).

4.2. Electrical Conductivity (EC)

The average electrical conductivity (EC) in the study area is 3877.31 µS/cm at 25 °C, indicating moderately high salinity (Figure 5). While the dissolution of minerals from the aquifer matrix contributes to the ionic composition and thus the EC of the groundwater, the primary cause of high EC in coastal areas is often seawater intrusion. Seawater typically has an EC greater than 50 mS/cm (50,000 µS/cm), considerably higher than the observed values in this study. However, even at lower concentrations, seawater intrusion can significantly impact groundwater quality. Factors such as over-extraction of groundwater and proximity to the coastline can exacerbate seawater intrusion, increasing the salinity of coastal aquifers. Further analysis, such as comparing ionic ratios to seawater or using isotopic tracers, is necessary to definitively determine the extent of seawater intrusion in the Témara Plain.

4.3. pH

The average pH value measured at 25 °C is 7.27, indicating slightly alkaline conditions (Figure 6). The pH of groundwater is controlled by a complex interplay of factors, including the dissolution of carbonate minerals (such as limestone and dolomite), cation exchange reactions, and the influence of dissolved CO_2 from the atmosphere and soil zone. The slightly alkaline pH observed in the Témara Plain is likely influenced by the dissolution of carbonate minerals, which releases calcium and bicarbonate ions into the groundwater, buffering the pH.

4.4. Calcium (Ca^{2+})

The average calcium concentration in the study area is 41.30 mg/L, which remains well below the World Health Organization (WHO) guideline of 200 mg/L for drinking water. However, this average masks significant spatial variability. Notably, elevated calcium levels were observed in the southwestern part of the Témara Plain, particularly around Sebbah and west of the Ain Attig and Sidi Yahya Zaër communes, with concentrations

reaching up to 123.4 mg/L (e.g., at sampling point Z50, Z51, Z52, Z53, and Z54). These localized increases are likely the result of geochemical interactions between groundwater and carbonate-rich geological formations, especially the dissolution of minerals such as calcite ($CaCO_3$) and dolomite ($CaMg(CO_3)_2$) and potentially gypsum ($CaSO_4$) from underlying evaporitic deposits.

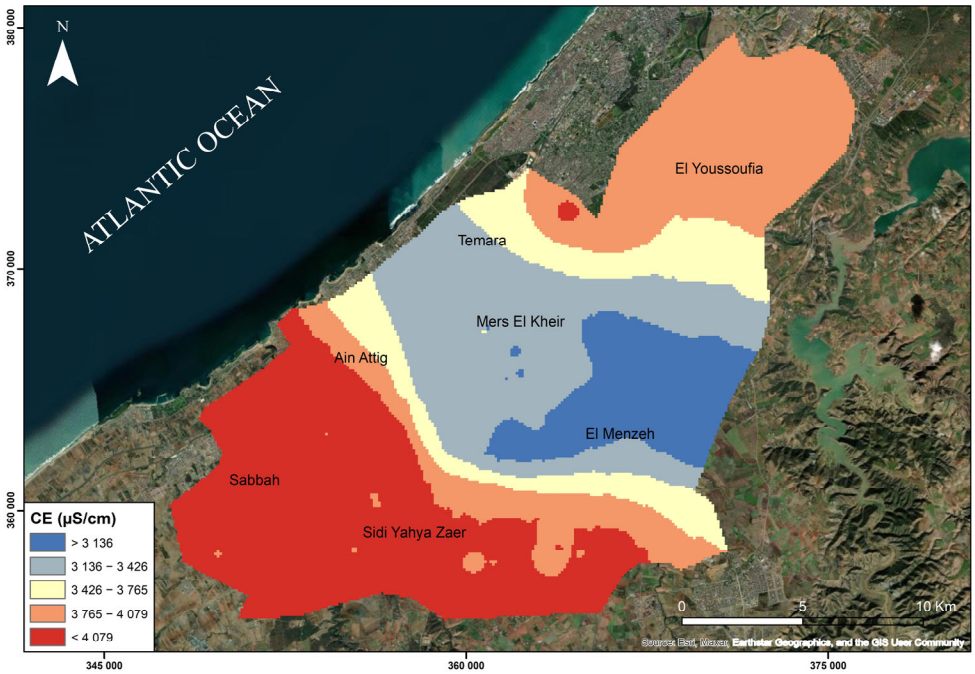

Figure 5. Spatial distribution of electrical conductivity (EC, µS/cm at 25 °C) in groundwater of the Témara Plain.

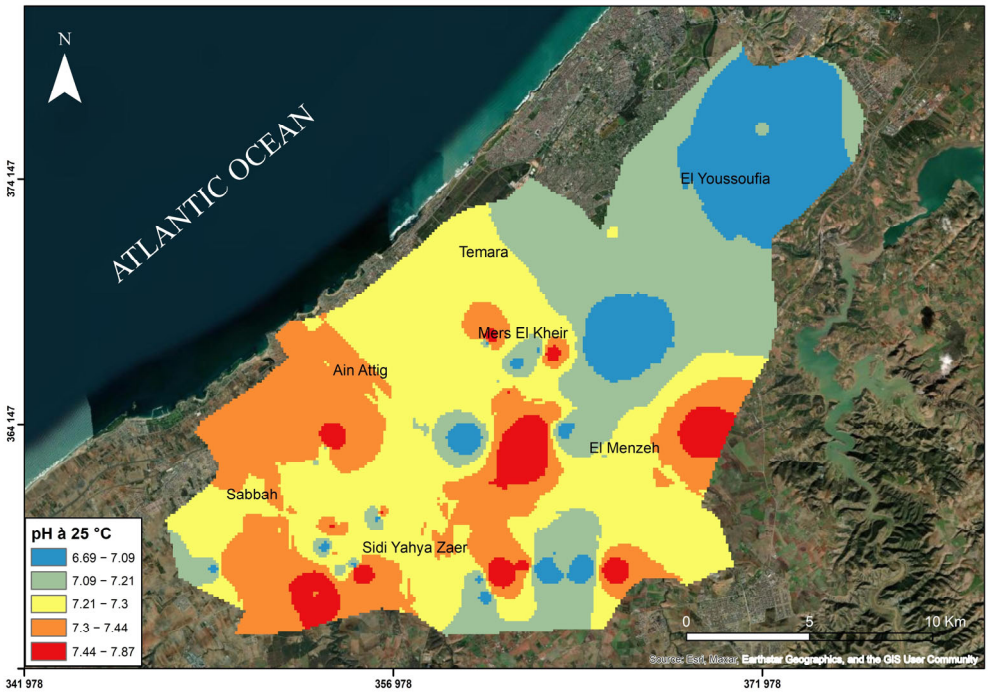

Figure 6. Spatial distribution of pH in groundwater of the Témara Plain.

These dissolution processes are often enhanced in areas with prolonged water–rock interaction and high permeability, which facilitate the mobilization of calcium into the

groundwater system. Although all measured concentrations remain within WHO limits, the locally elevated values may raise concerns regarding water hardness, which can lead to scale buildup in domestic plumbing and appliances, reduce irrigation efficiency, and negatively affect crop productivity, particularly for species sensitive to high hardness levels.

This spatial heterogeneity underscores the importance of implementing localized water quality monitoring strategies and targeted mitigation approaches to manage risks effectively. The spatial distribution of calcium concentrations and its geochemical interpretation are shown in Figure 7.

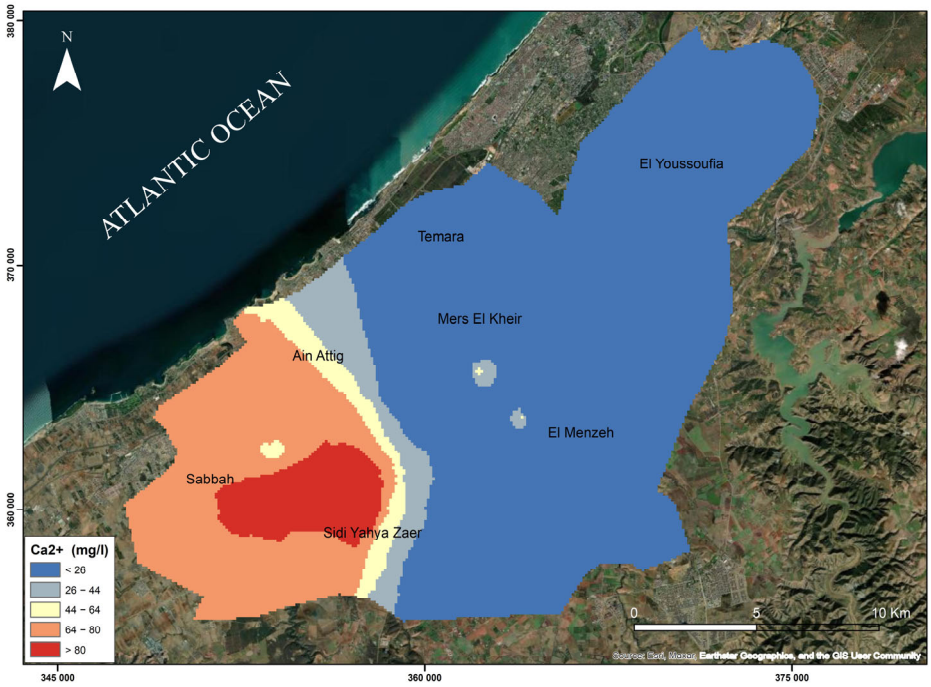

Figure 7. Spatial distribution of calcium (Ca^{2+}) concentrations in groundwater of the Témara Plain.

4.5. Potassium (K^+)

Figure 8 shows the spatial distribution of potassium concentrations in groundwater across the Témara Plain. Potassium (K^+), an essential nutrient for plant growth, is naturally abundant in minerals like potassium feldspars, micas, and clays. Soils in the region have an average K_2O content of approximately 3.2%. Potassium availability in soils is influenced by pH, with acidic soils generally exhibiting lower potassium levels compared to more basic soils. The primary sources of potassium in groundwater are the weathering of potassium-bearing minerals, particularly clay minerals, and the dissolution of potassium-rich fertilizers used in agriculture. In the study area, the highest potassium concentrations (55 mg/L) are observed in the southwestern part of Sidi Yahya Zaër, a region characterized by intensive agriculture. Agricultural practices, especially fertilizer application, contribute to elevated dissolved potassium in groundwater through leaching and irrigation return flow. However, the average potassium concentration across the Témara Plain is 26.82 mg/L, well below the WHO drinking water guideline of 200 mg/L. While localized agricultural inputs contribute to elevated potassium levels in certain areas, the overall impact on groundwater quality remains within acceptable limits.

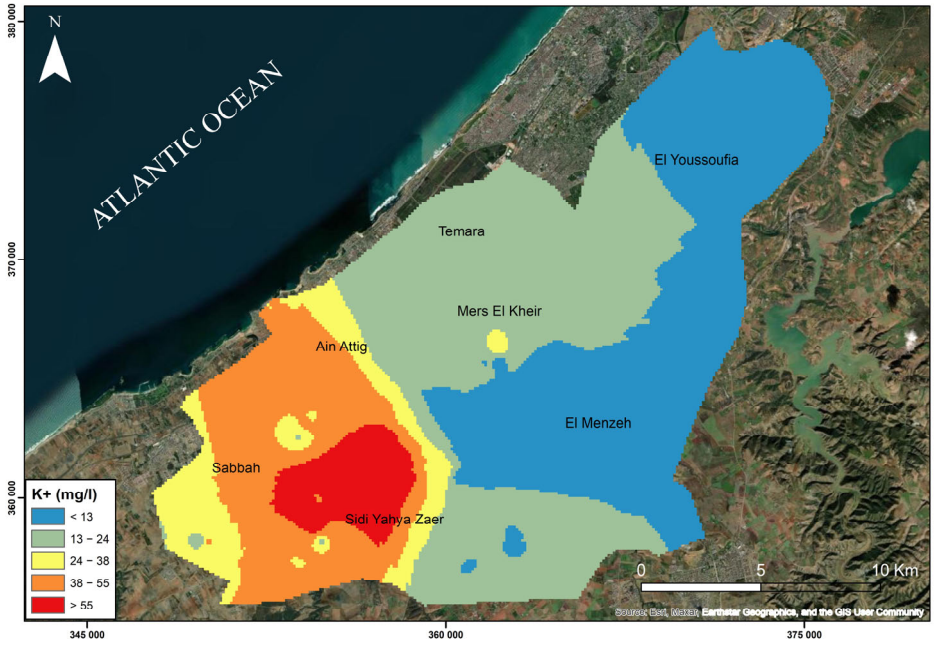

Figure 8. Spatial distribution of potassium (K^+) concentrations in groundwater of the Témara Plain.

4.6. Magnesium (Mg^{2+})

The average magnesium concentration in the Témara study area is 34.62 mg/L, which is below the WHO guideline limit of 50 mg/L for drinking water. However, spatial variability exists, with elevated concentrations observed in several wells, including Z34, Z37, Z39, Z40, Z41, Z42, Z43, Z46, Z47, Z48, Z49, Z50, Z51, Z52, and Z53 (Figure 9). Well Z51 exhibits the highest recorded calcium concentration at 123.4 mg/L. Several of these wells also show elevated magnesium levels. While initial observations suggest a trend of higher concentrations in the southwestern part of the aquifer, confirming this pattern requires further spatial analysis linking well IDs to specific locations (Figure 9). The elevated levels are likely due to the dissolution of dolomite ($CaMg(CO_3)_2$) and potentially gypsum ($CaSO_4 \cdot 2H_2O$) from the underlying geological formations, as well as potential seawater intrusion, suggested by the proximity to the coastline. Cation exchange, where sodium ions (Na^+) are replaced by magnesium ions (Mg^{2+}) from the groundwater, may also contribute to the observed magnesium concentrations. The observed magnesium levels in the groundwater across the region are generally suitable for human consumption.

4.7. Sodium (Na^+)

Sodium (Na^+) concentrations in the Témara Plain groundwater generally are below the WHO drinking water guideline of 200 mg/L. However, significant spatial variability exists, with elevated concentrations observed in several wells, reaching up to 360 mg/L at well Z5. This spatial variability is illustrated in Figure 10. Sodium in groundwater originates from various natural and anthropogenic sources, including evaporite dissolution, evaporation, and seawater intrusion. In coastal regions like the Témara Plain, seawater intrusion, particularly during low water levels, can substantially increase sodium concentrations in aquifers.

Rainfall leaching marine aerosols further exacerbates this process. The highest sodium concentrations are typically found near aquifer discharge points downstream, where saline intrusion is most pronounced due to reduced hydraulic head and tidal influence. In this study area, wells Z1, Z4, Z5, Z6, Z35, Z42, Z45, Z46, Z47, and Z51 exhibit sodium levels exceeding the WHO guideline. These wells appear clustered in central Mers El Khir, northern and northeastern El Menzah, and southwestern Sidi Yahya Zaër. Elevated

sodium levels pose challenges for domestic and agricultural water use. Excessive sodium in drinking water can be a health concern, while in irrigation water, it can lead to soil degradation, reduced infiltration, increased sodicity, and, ultimately, lower crop yields.

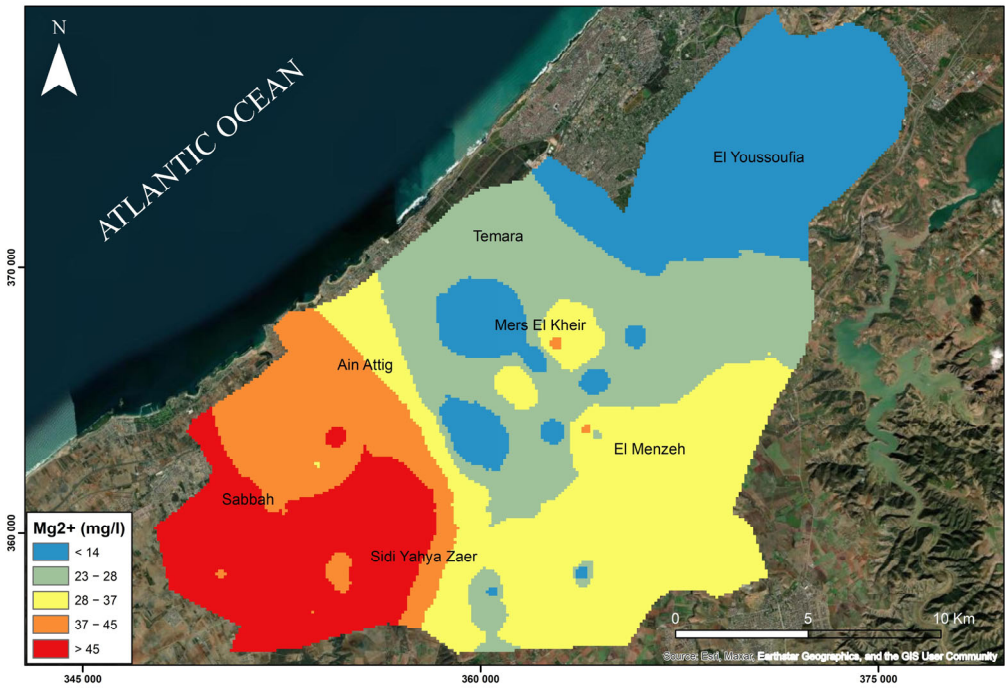

Figure 9. Spatial distribution of magnesium (Mg^{2+}) concentrations in groundwater of the Témara Plain.

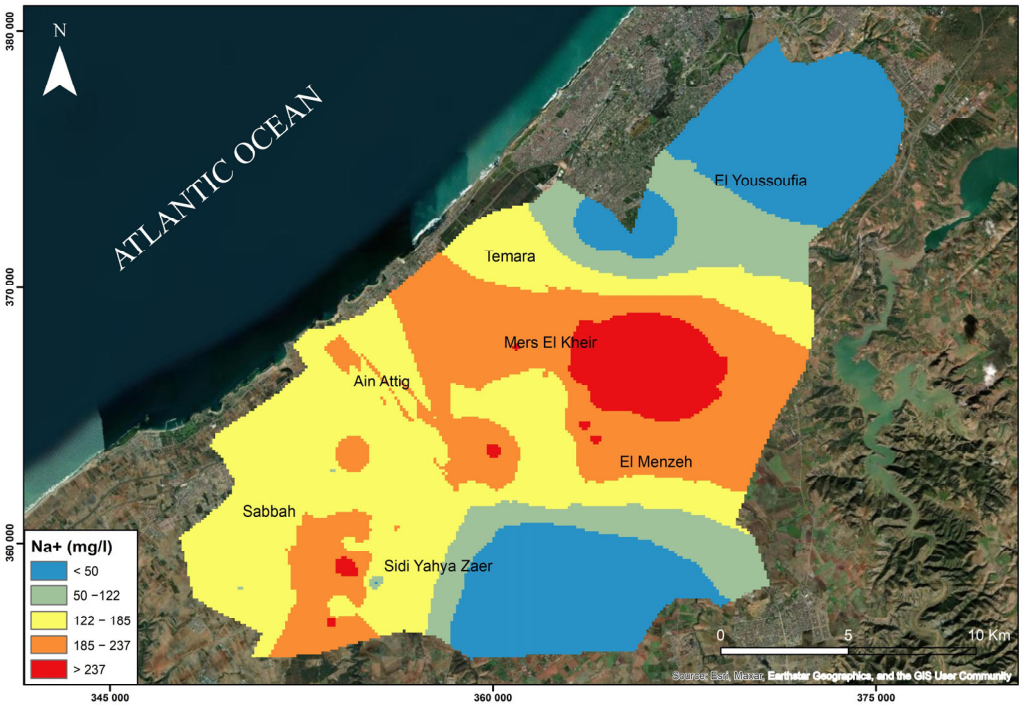

Figure 10. Spatial distribution of sodium (Na^{+}) concentrations in groundwater of the Témara Plain.

4.8. Chloride (Cl^{-})

Chloride (Cl^{-}), highly mobile in groundwater and resistant to adsorption or chemical reactions, serves as a useful tracer for water movement. Figure 11 illustrates the

spatial distribution of chloride concentrations in the Témara Plain. Key chloride sources include seawater intrusion, dissolution of chloride-bearing minerals in Paleozoic shales, and wastewater discharge. Elevated chloride levels (68.2 to 721 mg/L) were observed, with twenty wells exceeding the WHO drinking water guideline (250 mg/L): Z1, Z2, Z3, Z4, Z5, Z6, Z7, Z8, Z9, Z10, Z15, Z16, Z34, Z35, Z36, Z38, Z46, Z47, Z48, and Z49. These wells are primarily located in the northwestern coastal areas of Mers El Khir, Ain Attig, and Sebbah, concentrated in the northern portion of Sidi Yahya Zaër and also present in Témara and El Menzah. The regional average chloride concentration (349.60 mg/L) exceeds the WHO guideline. Excessive chloride in irrigation water can negatively impact crop yields by increasing salinity and reducing plant water availability. High chloride levels also contribute to infrastructure corrosion.

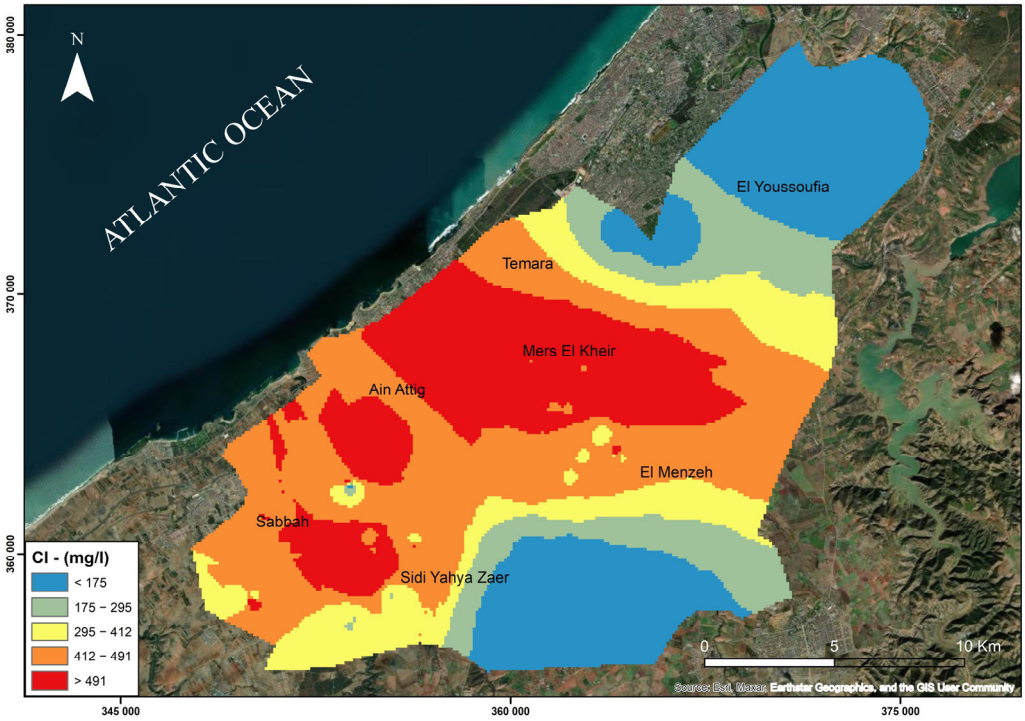

Figure 11. Spatial distribution of chloride (Cl^-) concentrations in groundwater of the Témara Plain.

4.9. Bicarbonate Ions (HCO_3^-)

Figure 12 illustrates the spatial distribution of bicarbonate (HCO_3^-) concentrations in the Témara Plain groundwater. The highest concentrations, exceeding 590 mg/L (well Z21), occur in the southeast and in wells near Sidi Yahya Zaër and Mers Elkhir. For example, high concentrations were found in wells Z21 (594 mg/L), Z4 (469 mg/L), Z5 (470 mg/L), Z6 (510 mg/L), and Z8 (452 mg/L). Bicarbonate in groundwater primarily originates from carbonate rock dissolution (e.g., limestone ($CaCO_3$) and dolomite ($CaMg(CO_3)_2$)). This occurs when CO_2-enriched water interacts with carbonate minerals, producing bicarbonate and calcium ions. Dissolved CO_2 forms carbonic acid (H_2CO_3), which dissociates into bicarbonate (HCO_3^-) and hydrogen (H^+) ions. This mechanism significantly influences the geochemical behavior of carbonate aquifers, affecting pH and mineral content. The elevated bicarbonate concentrations in these wells are primarily attributed to these water–rock interactions. While silicate mineral hydrolysis can also release bicarbonate, its contribution is likely less significant than carbonate dissolution in this context.

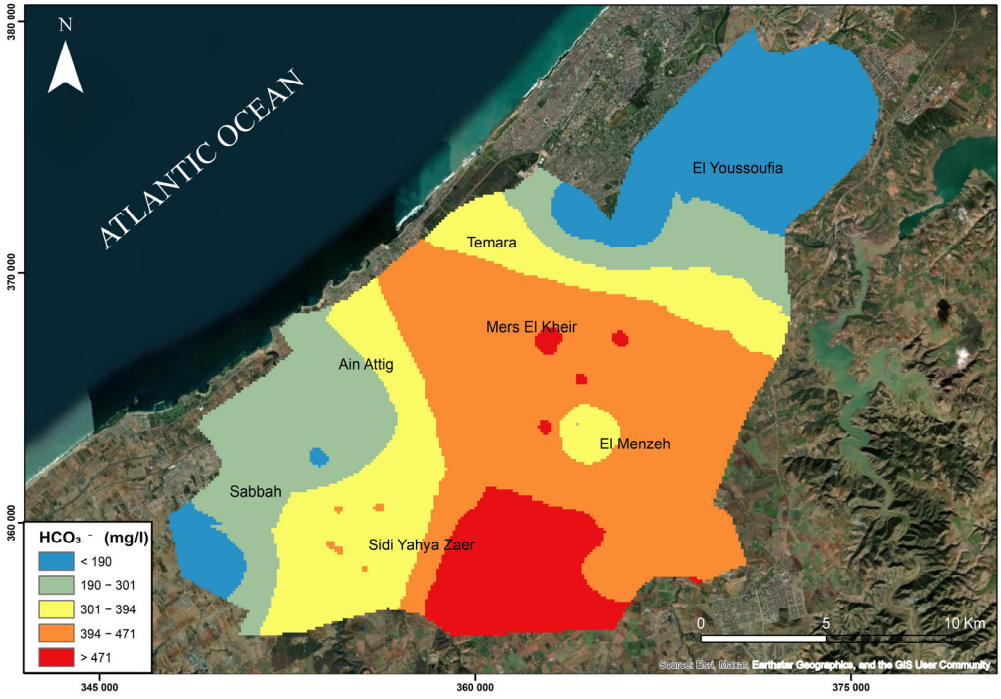

Figure 12. Spatial distribution of bicarbonate (HCO_3^-) concentrations) in groundwater of the Témara Plain.

4.10. Nitrates (NO_3^-)

Nitrate (NO_3^-) contamination in the groundwater of the Témara Plain is a significant environmental concern. The average recorded concentration reaches 50.22 mg/L, exceeding the World Health Organization (WHO) drinking water guideline of 45 mg/L. Figure 13 illustrates the spatial distribution of nitrate levels, highlighting elevated concentrations, particularly in the southwestern part of the plain. The highest values were observed in several wells, most notably well Z45, which recorded 152.3 mg/L, followed by Z38, Z46, Z36, and Z34, among others, all exceeding 84 mg/L. For instance, wells Z33 and Z35 to Z54, located between the Sebbah and Ain Attig areas, exhibit especially high nitrate concentrations, suggesting the presence of localized and persistent pollution sources. These regions (Sebbah, Ain Attig, and Sidi Yahya Zaër) are characterized by intensive agricultural activity, particularly in market gardening and, to a lesser extent, arboriculture, with heavy use of nitrogen-based fertilizers. In addition, the lack of adequate sanitation infrastructure, marked by the widespread use of non-collective systems, contributes to the infiltration of nitrogenous compounds into shallow aquifers, especially in peri-urban zones. While rainfall events may contribute to the leaching of nitrates, reducing their accumulation in the subsurface, periods of drought or low rainfall often lead to increased nitrate concentrations due to limited natural dilution and greater reliance on irrigation.

4.11. Sulfate (SO_4^{2-})

Sulfate (SO_4^{2-}) concentrations in the Témara Plain groundwater generally remain below the WHO drinking water guideline of 250 mg/L, with an average concentration of 40.93 mg/L. However, spatial variability exists. The highest concentrations, exceeding 70 mg/L, are observed in wells Z55, Z56, Z57, and Z58, located in the northern and northeastern regions of the study area (Figure 14). The primary source of sulfate in the groundwater is the natural dissolution of gypsum ($CaSO_4^-$ $2H_2O$). However, anthropogenic activities, such as urban discharges at the mouth of the Oued Bouregreg and the use of sulfate-containing fertilizers in agriculture, also contribute to sulfate enrichment.

The combined effects of these natural and anthropogenic sources result in the observed sulfate distribution.

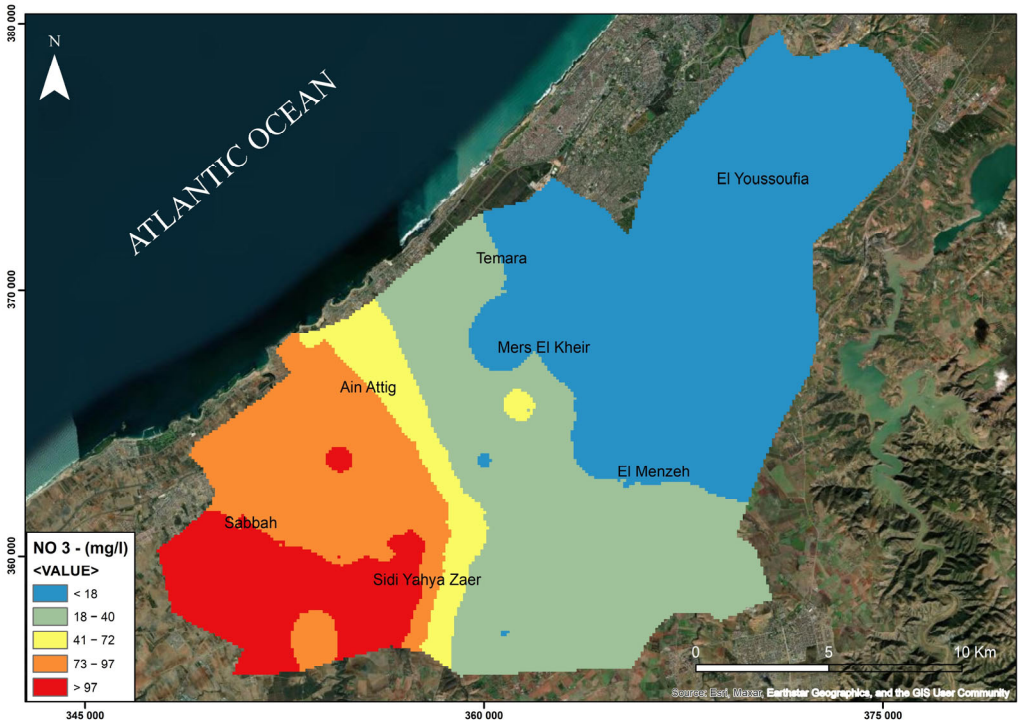

Figure 13. Spatial distribution of nitrate (NO_3^-) concentrations in groundwater of the Témara Plain.

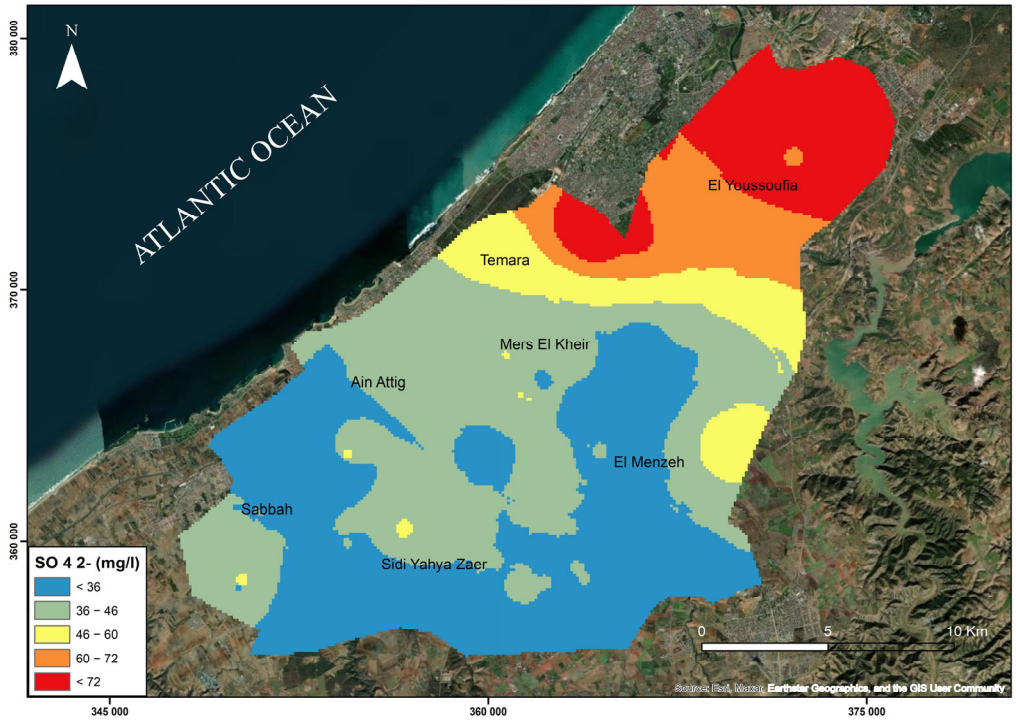

Figure 14. Spatial distribution of sulfate (SO_4^{2-}) concentrations in groundwater of the Témara Plain.

4.12. Principal Component Analysis (PCA) of Hydrochemical Data

Principal component analysis (PCA) was applied to the hydrochemical data (Table 4) to identify the dominant factors influencing groundwater chemistry in the Témara Plain. Table 5 presents the eigenvalues and explains the variance for each principal component.

The first two components (F1 and F2) account for 61.87% of the total variance, capturing the major hydrochemical trends. Figure 15 shows the variable biplot in the F1–F2 factorial plane. Component F1 (40.69% variance) is primarily associated with Ca^{2+}, Mg^{2+}, K^+, NO_3^-, and electrical conductivity (EC). This component likely represents a mineralization gradient influenced by both natural water–rock interactions (carbonate mineral dissolution) and anthropogenic inputs (agricultural fertilizers). The positive association of NO_3^- with Ca^{2+}, Mg^{2+}, and EC suggests that agricultural activities contribute significantly to groundwater mineralization. Component F2 (21.18% variance) exhibits a strong correlation with Na^+ and Cl^-, indicating saline water intrusion into the coastal aquifer. This intrusion is likely driven by groundwater over-extraction and proximity to the Atlantic Ocean. Component F3 (13.23% variance) reveals an inverse relationship between HCO_3^- and SO_4^{2-}, suggesting competing processes: carbonate mineral dissolution (increasing HCO_3^-) and sulfate-rich sources (e.g., sulfide oxidation or anthropogenic inputs) [38]. Component F4 (10.09% variance), dominated by pH, likely reflects carbonate equilibrium reactions. Component F5 (5.79% variance) shows an association between K^+ and HCO_3^-, potentially related to the weathering of potassium-bearing silicate minerals.

Table 5. Eigenvalues and variance explained by principal components for hydrochemical parameters.

	F1	F2	F3	F4	F5	F6
Eigenvalue	4.069	2.118	1.323	1.009	0.579	0.279
Variability (%)	40.692	21.180	13.228	10.089	5.793	2.790
Cumulative %	40.692	61.872	75.100	85.189	90.982	93.773

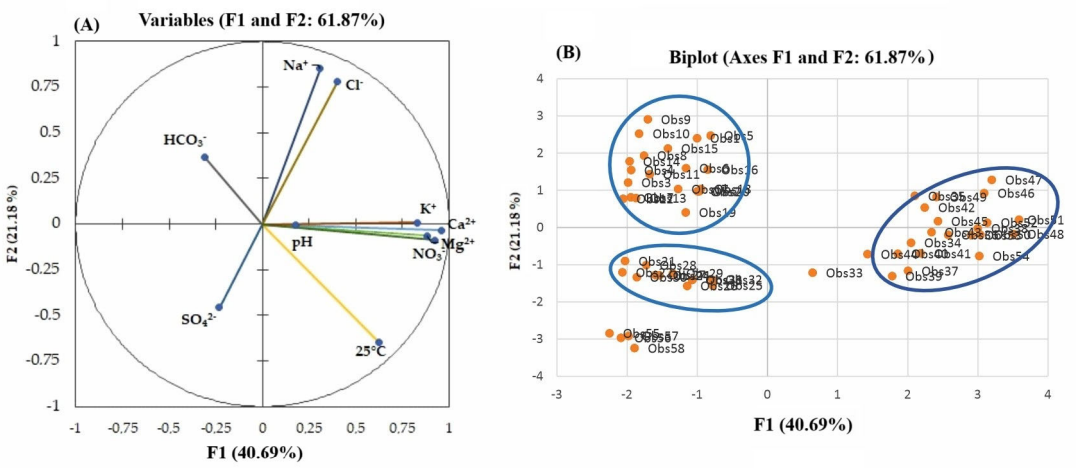

Figure 15. (**A**) Biplot of variables and samples in the plane defined by the first two principal components (F1 and F2) for hydrochemical parameters, illustrating the relationships between variables and the grouping of samples into distinct clusters; (**B**) factorial validation diagram F1–F2.

4.13. Vulnerability Map

The intrinsic groundwater vulnerability of the Témara aquifer was spatially assessed using the DRASTIC model, yielding the vulnerability map presented in Figure 16 (bottom right panel). The DRASTIC index (DI) was derived from the integration of seven hydrogeological parameters (D, R, A, S, T, I, C), whose individual spatial distributions are also depicted in Figure 16 and whose respective standard weights and rating ranges are detailed in Table 3. The resultant groundwater vulnerability map for the Témara Plain (Figure 16, DRASTIC map) illustrates a significant spatial heterogeneity in the aquifer's intrinsic susceptibility to contamination. Analysis of this map (Figure 16, DRASTIC map) indicates that areas classified as "Very High" and "High" vulnerability are predominantly concentrated in the Ain Attig, Sabah, Sidi Yahya Zaer, and parts of El Youssoufia sectors.

Zones exhibiting "Moderate" vulnerability include Témara, Mers El Kheir, and El Menzeh. Conversely, "Low" to "Very Low" vulnerability characterizes the southeastern portion of the plain.

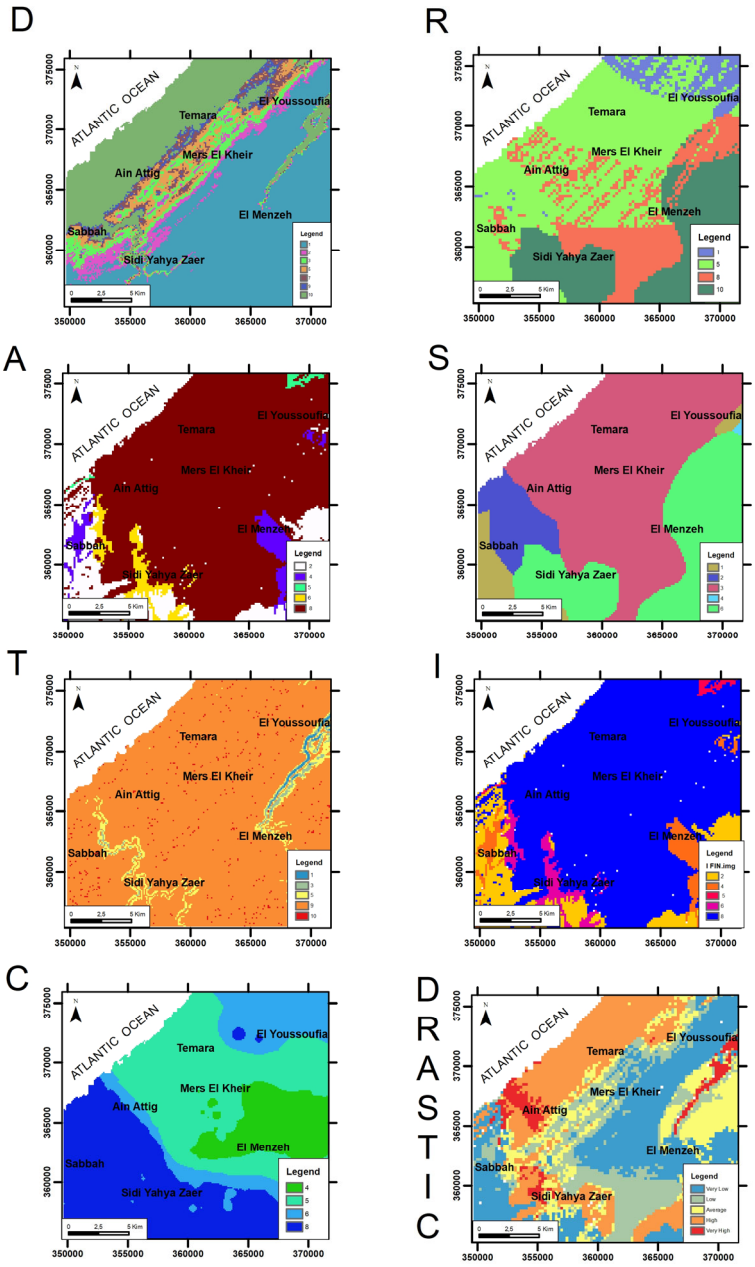

Figure 16. Groundwater vulnerability map of the Témara aquifer derived from the DRASTIC model.

5. Discussion

5.1. Geological and Anthropogenic Controls on Groundwater Hydrochemistry

The groundwater chemistry of the Témara Plain is shaped by a complex interaction between natural geological processes and anthropogenic activities. The region's sandy and carbonate formations promote ion exchange and mineral dissolution, establishing the baseline hydrochemical signature. This aligns with broader understandings of hydrogeochemical processes, as similar interactions influencing groundwater chemistry have been observed in various geological settings [66,67]. However, human activities, particularly intensive agriculture, substantially alter this natural baseline [68]. Elevated nitrate and potassium concentrations observed in areas with extensive agricultural land use

(Figures 8 and 13 and Table 3) directly correlate to fertilizer application and irrigation return flows [69]. This finding is consistent with global observation of agricultural fertilizing practices' impacts on groundwater quality. Boualem and Egbueri [70] used graphical, statistical, and index-based techniques to identify hydrochemical fingerprints and origins of groundwater quality parameters in northwest Algeria, demonstrating how agricultural activities can significantly alter groundwater quality. Likewise, studies by Liu et al. [71] and Zheng et al. [72], using multivariate statistical analysis and inverse geochemical modeling, identified agricultural practices and the dissolution of evaporites as key factors influencing shallow groundwater composition across different regions. Increased sodium and chloride concentrations in coastal areas of the Témara Plain (Figures 10 and 11 and Table 3) suggest the influence of seawater intrusion, a common issue in coastal aquifers exacerbated by overextraction. Kuriqi and Abd-Elaty [32] assessed the risk of earthquake-induced saltwater intrusion affecting groundwater salinity in coastal regions, emphasizing the vulnerability of these areas to natural events. Wijerathne et al. [73], studying the Marawila coastal zone in Sri Lanka, found that hard coastal engineering structures significantly impacted groundwater salinity and intrusion patterns, demonstrating the influence of human interventions on coastal aquifer dynamics. The combined effects of these natural and anthropogenic influences underscore the need for integrated water resource management strategies in the Témara Plain.

- The Influence of Geological Formations on the Chemical Composition of Water

The local geological formations play a critical role in shaping the chemical composition of groundwater. In some sectors, such as Ain Attig, Mers El Khir, and Sidi Yahya Zaër, the groundwater shows elevated ion concentrations of chlorides, sodium, and potassium. These higher values can be explained by the presence of rocks like sands (Figure 17a), sandstones, and calcarenites (Figure 17b,c), promoting the dissolution of soluble salts (chlorides, sodium, and potassium sulfates), thereby increasing their concentration in the aquifers. This geochemical mechanism has been extensively described in the hydrogeochemical literature [47]. Furthermore, regional studies in Morocco [74,75] and Malawi [76] have confirmed that sandy and alluvial formations in contact with salt-rich layers act as natural vectors of salinization via the mobilization of chlorides and other dissolved ions.

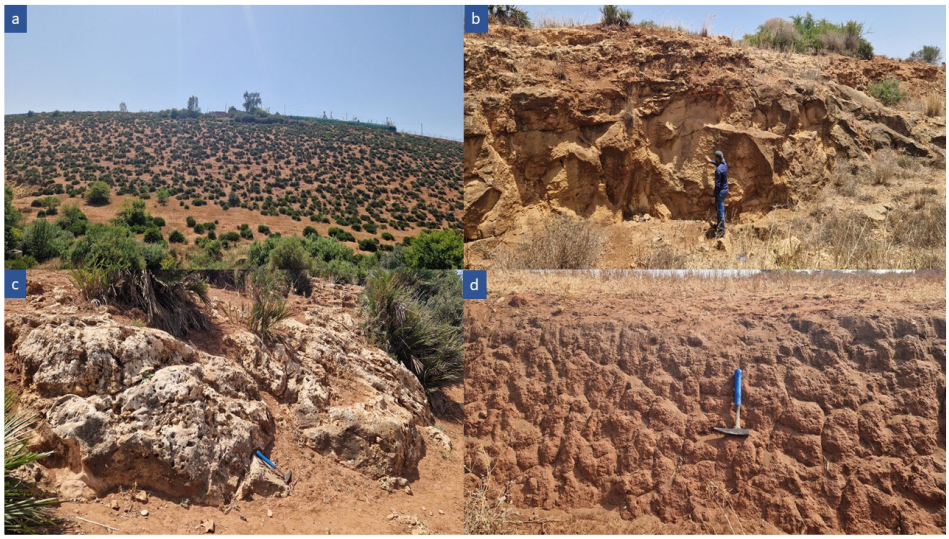

Figure 17. Geological diversity of outcropping rocks in the study area. (**a**) Cenozoic cover showing thickness up to 40 m in the central area; (**b**) thick-bedded calcarenite beneath sandy–clay soil; (**c**) conglomeratic to sandy limestone showing dissolution features; (**d**) sandy–clay beds of the Cenozoic cover.

In contrast, areas like Sebbah and El Youssoufia are dominated by clay and marl formations (Figure 17d), which primarily release calcium and magnesium. This highlights the significant impact of local geology on the chemical nature of groundwater, which can have implications for water quality, particularly for human consumption and agricultural purposes.

- Factors Influencing Groundwater Contamination in the Témara Aquifer

The intrinsic vulnerability assessment of the Témara aquifer, culminating in the DRASTIC map (Figure 16), delineates distinct spatial patterns of susceptibility. These patterns are directly attributable to the interplay between local hydrogeological characteristics, as represented by the individual DRASTIC parameter maps and their consequent influence on contaminant transport pathways. Zones identified with "Very High" and "High" vulnerability—notably Ain Attig, Sabah, Sidi Yahya Zaer, and portions of El Youssoufia—are interpreted as areas where hydrogeological settings are inherently conducive to contamination. Such settings typically exhibit shallow water tables (high D-parameter rating), permeable aquifer and soil media (high A- and S-parameter ratings), and/or significant recharge rates (high R-parameter rating), as indicated by the respective parameter maps (Figure 16). These intrinsic hydrogeological conditions render the aquifer particularly susceptible to the prevailing anthropogenic pressures within these zones. Key pressures include intensive agricultural practices reliant on nitrogen-based fertilizers, rapid urban expansion often outpacing the development of comprehensive sanitation infrastructure, and the widespread presence of unconnected wastewater systems in peri-urban locales. Collectively, these factors can significantly facilitate the percolation of nitrogenous and microbial contaminants into the vulnerable shallow aquifer. Moreover, the existence of unregulated waste dumps and informal waste storage sites within these vulnerable areas further exacerbates the risk of localized pollution.

In sectors categorized as "Moderate" vulnerability, such as Témara, Mers El Kheir, and El Menzeh, the hydrogeological conditions, while less critical, still pose a notable risk. Here, contamination threats are frequently linked to urban runoff (Figure 18), potential seawater intrusion (particularly in coastal areas with conducive hydrogeological pathways), inadequate stormwater management systems, and relatively permeable soils, all of which can promote pollutant infiltration. Conversely, areas demonstrating "Low" to "Very Low" vulnerability, predominantly situated in the southeastern part of the plain, generally coincide with sparsely populated or forested regions. These areas likely benefit from protective hydrogeological features. These may include a greater depth to groundwater (low D-parameter rating), less permeable vadose zone or aquifer materials (low A-, S-, or I-parameter ratings), or diminished recharge rates (low R-parameter rating), as suggested by the individual parameter maps (Figure 16). Such features collectively establish a more effective natural barrier, thereby limiting contaminant transport. This comprehensive vulnerability assessment, therefore, serves as a critical decision-support tool. It is instrumental in guiding the prioritization of groundwater protection strategies, such as the targeted expansion of sanitation networks, the regulation of fertilizer application in highly vulnerable agricultural zones, the enhancement of solid waste management practices, and the implementation of focused groundwater quality monitoring programs, particularly in high-risk areas.

Beyond intrinsic vulnerability, groundwater quality in specific regions like Sidi Yahya Zaër, Ain Attig, and Mers El Khir is demonstrably impacted by a confluence of pollution sources. While intensive agriculture (Figure 18A,B), particularly market gardening and, to a lesser extent, arboriculture, is a major contributor to elevated nitrate concentrations due to the excessive application of nitrogenous fertilizers, it is not the sole determinant of water quality degradation. In areas where irrigation utilizes water with high dissolved solids

content, an increase in sodium and chloride levels is often observed. This phenomenon can lead to elevated electrical conductivity and, in some cases, reduced alkalinity in the groundwater, particularly where bicarbonate enrichment is limited.

Figure 18. Anthropogenic pressures contributing to groundwater pollution in the Témara Plain. (**A**) Intensive agriculture on permeable soils; (**B**) cereal cultivation on expansive agricultural land; (**C**) discharge of untreated urban wastewater in Sidi Yahya Zaër; (**D**) stream channel affected by urban runoff in the Sabah area.

Furthermore, the influence of land use on nitrate pollution, as illustrated in Figure 19, underscores the role of urban and peri-urban activities in exacerbating water quality issues (Figure 18C,D). Wastewater discharges from several urban and peri-urban centers (e.g., Sebbah, Ain Attig, and Sidi Yahya Zaër) tend to flow toward topographically low-lying areas. This facilitates the infiltration of organic nitrogen compounds and other pollutants, substantially increasing nitrate concentrations, especially in aquifers with limited natural protection. An additional significant concern is the potential for leachate generation from household waste disposed of in informal dumping sites, which typically lack engineered containment or treatment infrastructure. These sites represent potent localized sources of contamination by nitrogenous compounds and a spectrum of other pollutants.

Finally, climatic factors also modulate contamination processes. Although precipitation can, under favorable conditions, contribute to the reduction in nitrate accumulation through natural leaching and dilution, recurrent drought periods diminish this natural attenuation capacity. Consequently, increased reliance on irrigation during dry spells can inadvertently intensify the accumulation of contaminants within shallow aquifer systems.

- Marine Intrusion

Seawater intrusion significantly impacts groundwater quality in coastal areas of the Témara Plain. Elevated sodium (Na^+) and chloride (Cl^-) concentrations, characteristic of seawater, are observed in wells located near the coastline, particularly in Mers El Khir and Ain Attig. As evidenced by wells Z1, Z4, and Z5, located near the coast, exhibit sodium concentrations exceeding the WHO drinking water standard of 200 mg/L, reaching up to 360 mg/L at well Z5. Similarly, chloride concentrations surpass the 250 mg/L WHO threshold in several coastal wells, reaching up to 721 mg/L, rendering the water unsuitable for both human consumption and irrigation [77]. This localized increase in salinity,

indicative of seawater intrusion, is likely exacerbated by excessive groundwater extraction, which brings down the freshwater head, enabling landward migration of saline water. The Témara Plain's proximity to the Atlantic Ocean further enhances its vulnerability to seawater intrusion. According to the theoretical Ghyben–Herzberg model [78], the density difference between freshwater and seawater implies that a one-meter decline in the water table can cause the saltwater interface to rise approximately 40 m upward. Consequently, any lowering of the water table promotes seawater infiltration into freshwater-bearing layers, especially in zones characterized by high permeability, such as sandy or gravelly formations. The strong loading of Na^+ and Cl^- on principal component F2 confirms the geochemical influence of seawater intrusion in coastal areas. This salinization process affects groundwater to varying extents depending on aquifer depth. Shallow layers, typically more permeable and located closer to the shoreline, are more prone to rapid and widespread intrusion. Although deeper aquifers may initially be less affected, they remain at risk due to the pressure drop caused by excessive pumping. This reduction in hydraulic pressure weakens the ability of freshwater to counterbalance seawater intrusion, eventually allowing salinity to penetrate deeper layers.

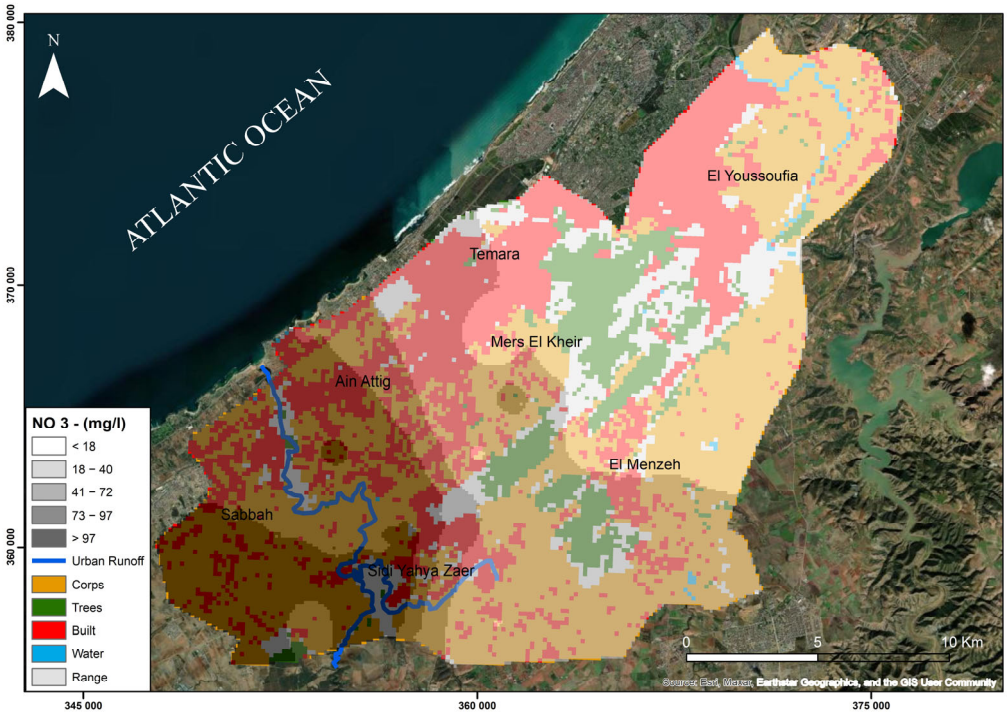

Figure 19. Land-use influence on nitrate pollution in groundwater.

Furthermore, seawater intrusion can increase concentrations of other alkaline earth metals, such as calcium (Ca^{2+}) and magnesium (Mg^{2+}), as a result of chemical interactions with minerals in sandy or carbonate formations. This alters the chemical composition of groundwater, reducing its suitability for drinking and irrigation and impairing soil fertility. The intrusion also disrupts ionic equilibrium, notably the relationship between bicarbonates (HCO_3^-) and sodium (Na^+), which may enhance water corrosiveness, damaging infrastructure such as pipes. This is particularly concerning for agriculture, as the use of such water can lead to soil salinization and decreased agricultural productivity [79].

The progressive intrusion of seawater reduces the availability of freshwater in coastal aquifers, significantly impacting water resources. This renders the groundwater unsuitable for domestic consumption or irrigation, thereby affecting water supply for both agricultural and household uses and potentially leading to localized water crises. Moreover, increased

groundwater salinity has serious repercussions on local ecosystems, particularly in terms of agriculture and freshwater-dependent vegetation. Plants exposed to saline conditions may experience salt stress, stunted growth, or even die, which negatively affects soil productivity and agricultural yield. Additionally, the natural habitats of flora and fauna that rely on freshwater may be disrupted, threatening ecological balance and increasing ecosystem vulnerability to climate change.

Recent research has highlighted the significance of integrating dynamic geophysical factors, such as earthquakes, into assessments of the vulnerability of coastal aquifers to seawater intrusion. Seismic events can induce sudden changes in groundwater pressure and aquifer permeability, significantly advancing the inland movement of the saltwater front. Numerical simulations have demonstrated that even a horizontal ground acceleration of 0.1 g can cause the inland progression of saline intrusion by several hundred meters, especially in regions already impacted by excessive groundwater abstraction and rising sea levels [32]. The seismic factor holds particular relevance in the Moroccan context, where the country lies along the boundary of an active tectonic zone between the African and Eurasian plates. While the Témara region is not considered one of the areas most exposed to high seismic activity, its historical record includes moderate earthquakes that should not be overlooked when developing long-term hazard scenarios [80]. Therefore, including potential seismic impacts in the hydrogeological assessment of the Témara aquifer is crucial to understanding the complex interactions between natural and anthropogenic pressures—especially in light of increasing abstraction rates and declining natural recharge. It is thus recommended that future coastal water management strategies in Morocco, particularly in the Témara region, incorporate seismic scenarios into predictive models of saltwater intrusion and groundwater quality evolution.

- Contextualizing Témara Groundwater Quality: National and Regional Comparisons

The hydrogeochemical characteristics and controlling factors identified in the Témara Plain aquifer, such as its susceptibility to salinization and diverse anthropogenic impacts, resonate with findings from other semi-arid regions in Morocco and the broader Mediterranean basin [26,81–84]. The challenges of groundwater quality degradation observed in Témara are mirrored in various regional contexts. For example, Argamasilla et al. [81] investigated coastal aquifers in southern Spain, a region also facing water stress. Similar to our study in Témara, their work highlighted the influence of diverse source lithologies on groundwater geochemistry and employed integrated hydrogeochemical and statistical methods. However, a key distinction is that active saline intrusion was found to be negligible in their specific study area at the time of sampling, with salinity variations attributed more to mixing with other water sources and past events, whereas in Témara, active seawater intrusion (Component F2) is a dominant current process. This comparison underscores the importance of site-specific assessments even within regions facing similar overarching pressures and validates the utility of integrated approaches in diverse coastal settings.

In Ain Djacer, Eastern Algeria, Ziani et al. [82] identified hydrochemical facies (Ca-HCO_3 inland, SO_4-Na in discharge zones) and pollution sources analogous to Témara's Ca-HCO_3 inland and Na-Cl coastal facies. Their PCA/FA findings also resonated with ours, revealing primary "salinization" and secondary "agricultural contamination" factors. The main difference lies in the primary salinization driver: evaporite dissolution was more pronounced in Ain Djacer, while direct seawater intrusion is key in coastal Témara. Nonetheless, both studies highlight the significant impact of agricultural activities on nitrate levels and the efficacy of statistical methods in distinguishing natural mineralization from anthropogenic pollution. Similarly, research in other North African agricultural basins, such as the Maknessy Basin in central Tunisia by Moussaoui et al. [83], reveals common challenges. Both Témara and Maknessy are heavily reliant on groundwater for irrigation

and utilize comparable hydrochemical and statistical approaches (PCA, HCA). While dominant water types differ due to local geology (e.g., Ca-hyper chloride and Ca-sulfate in Maknessy vs. Na-Cl and Ca-HCO_3 in Témara), both studies identify mineralization (high EC/TDS) and agricultural pressures as principal concerns. Although our current work did not include isotopic analysis, which Moussaoui et al. used to confirm recharge and evaporation effects, both investigations underscore the critical need for sustainable groundwater management in Mediterranean agro-ecosystems.

Within Morocco, the findings of Nassri et al. [26] in northwestern Morocco also point to lithological diversity as a key control on groundwater chemistry. While both studies effectively used Piper diagrams and GIS for spatial analysis, Témara exhibited distinct coastal Na-Cl facies due to seawater intrusion and more widespread agricultural nitrate pollution compared to the Ca-Mg-Cl and Ca-Mg-HCO_3 facies with localized nitrate contamination reported by Nassri et al. This suggests that anthropogenic pressures may be more pronounced and diverse in the Témara Plain. Further comparison with the Kourimat aquifer system (Essaouira basin), studied by Bahir et al. [84], also provides valuable context. Their work detailed groundwater dynamics and classified water types in dolomitic limestone and marl–limestone aquifers. Analogous to Témara, the Kourimat system's groundwater chemistry is influenced by its carbonate lithology. While Bahir et al. focused on hydraulic gradients and seasonal fluctuations, and our study emphasized specific anthropogenic pollution signatures like elevated nitrates and chlorides (identified via IDW mapping), both investigations highlight the vulnerability of Moroccan aquifers to both natural mineralization processes and human activities, underscoring the importance of proactive monitoring and mitigation.

Collectively, these comparisons situate Témara's hydrogeochemical challenges within a broader regional framework. They illustrate commonalities in natural processes and anthropogenic pressures across Mediterranean and Moroccan aquifers while also emphasizing the site-specific geological and socio-economic factors that define Témara's unique vulnerability profile and inform targeted management strategies.

5.2. Water Resource Management, Socio-Economic Impacts, and Environmental Health

5.2.1. Issues and Impacts on Water Resources in the Témara Plain

The Témara region faces critical groundwater management challenges driven by demographic growth and urban expansion. Groundwater reserves constitute a major source of water in the region, supporting essential needs such as drinking water supply, agricultural irrigation, and industrial activities [85]. However, overexploitation has triggered an alarming water table decline of approximately 1 to 2 m per year in some areas [86]. Seawater intrusion poses a major threat to water quality, particularly in coastal areas such as Mers El Khir and Ain Attig, where chloride concentrations occasionally exceed 300 mg/L, surpassing the WHO guideline of 250 mg/L. Concurrently, nitrate pollution from agricultural activities is another major concern: in some farming districts, nitrate concentrations range between 70 and 150 mg/L, far exceeding the recommended limit of 50 mg/L for drinking water [87]. The socio-economic consequences of these issues are substantial. The deterioration of water quality leads to increased costs for drinking water treatment and the implementation of alternative supply solutions. Additionally, soil salinization resulting from irrigation with poor-quality water reduces agricultural productivity, directly impacting farmers' incomes.

5.2.2. Sustainable Management Strategies and Best Practices

To safeguard groundwater resources in the Témara region, a multifaceted approach is essential. Implementing artificial aquifer recharge through infiltration basins and the

reuse of treated wastewater can help offset losses caused by over-extraction. Effective implementation methods for these strategies include the construction of infiltration basins in sandy or highly permeable areas, the use of direct injection wells in urban zones or in low-permeability geological formations, and the reuse of tertiary-treated wastewater for agricultural irrigation or artificial aquifer recharge. In the Témara Plain, the geological setting characterized by sandy layers and shallow groundwater offers favorable conditions for applying these solutions, particularly in the southern areas of Ain Attig and Sebbah. This requires enhancing the capacity of the Témara wastewater treatment plant or establishing decentralized treatment units, along with the development of a legal and regulatory framework to ensure safe and high-quality water reuse practices.

Additionally, optimizing irrigation techniques, such as adopting drip and deficit irrigation, would significantly reduce water consumption while ensuring stable agricultural yields. A more integrated wastewater management system, including the expansion of treatment plants and the reuse of treated wastewater for irrigation, would also alleviate pressure on groundwater reserves. Furthermore, establishing real-time monitoring and early warning systems would enable authorities to track fluctuations in groundwater levels and quality, allowing for proactive risk mitigation. Lastly, raising awareness among farmers and industrial stakeholders through educational initiatives on sustainable water management practices would foster a culture of conservation and responsible usage, ultimately ensuring the long-term sustainability of this vital resource. These strategies have been successfully implemented in other similar regions. For instance, in Agadir, a pilot project for artificial aquifer recharge using treated wastewater has improved groundwater availability and mitigated seawater intrusion [88].

These strategies have already been successfully implemented in other regions with comparable hydrogeological and climatic conditions. For instance, a pilot project in Agadir demonstrated that artificial aquifer recharge using treated wastewater significantly improved groundwater availability and mitigated seawater intrusion [89]. Similarly, the Souss-Massa region has adopted localized irrigation techniques and artificial recharge in parallel with the reuse of treated wastewater for agricultural purposes, which has contributed to stabilizing groundwater levels and mitigating the effects of drought [90]. In alignment with the priorities outlined in Morocco's National Water Plan 2020–2050 (PN-Eau), our study directly contributes to the achievement of national objectives concerning the sustainable management of water resources. The PN-Eau emphasizes the need for innovative strategies to address challenges related to water scarcity, climate change, and increasing water demand, particularly in vulnerable coastal areas such as the Témara Plain. In this context, the recommendations derived from our study, such as artificial aquifer recharge using treated wastewater and the adoption of efficient irrigation techniques like drip irrigation, are fully in line with the PN-Eau's goals to protect groundwater resources and alleviate the pressure on these resources. Furthermore, integrating practices such as the reuse of treated wastewater for irrigation and developing real-time monitoring systems to track groundwater levels aligns directly with the PN-Eau's strategies for promoting Integrated Water Resources Management (IWRM) [90]. Thus, the findings of our study provide valuable insights for implementing the actions outlined in the PN-Eau, offering practical solutions for ensuring the sustainability of water resources in the Témara region and, more broadly, in other areas of Morocco facing similar challenges.

5.2.3. Stakeholder Engagement and Collaboration

Sustainable groundwater management is a collective responsibility that requires the collaboration of multiple stakeholders, each playing a crucial role in protecting and efficiently using this vital resource. Government authorities and water management organiza-

tions, such as the Ministry of Equipment and Water and regional basin agencies, are at the forefront of shaping water policies, enforcing regulations, and funding projects aimed at aquifer recharge and infrastructure improvement [91]. Meanwhile, farmers and the agricultural sector, as major consumers of groundwater, must adopt water-saving techniques like drip irrigation and eco-friendly fertilizers. Providing training programs and financial incentives can support their transition to more sustainable practices, reducing both overuse and pollution [88]. Similarly, industries and businesses, particularly in the agri-food and manufacturing sectors, must minimize their impact by implementing water recycling systems and adhering to stricter environmental policies to prevent contamination [92]. At the community level, local residents and civil society play a key role in groundwater conservation. Raising awareness about responsible water use, minimizing waste, and actively involving communities in sustainability initiatives can significantly strengthen long-term resource preservation [93,94]. By fostering cooperation among these key players, we can ensure a more resilient and sustainable groundwater management system.

This study provides a crucial baseline assessment of groundwater quality in the Témara Plain, but further research is needed to refine our understanding and optimize management strategies. Future investigations could explore (1) the use of isotopic tracers to quantify the contribution of different sources to groundwater recharge and salinization; (2) the development of predictive groundwater models to assess the long-term impacts of climate change and land-use changes on water resources; and (3) the evaluation of the effectiveness of different management interventions, such as artificial recharge and modified agricultural practices, on improving groundwater quality. This research also highlights the importance of community engagement and stakeholder collaboration in developing and implementing sustainable water management solutions. By fostering a participatory approach, we can ensure that management strategies are not only scientifically sound but also socially equitable and economically viable, promoting the long-term health and resilience of the Témara Plain's vital groundwater resources.

6. Conclusions

This study investigated the groundwater quality of the Témara Plain, revealing a complex interplay of natural and anthropogenic factors impacting its suitability for various uses. Specifically, addressing the research questions posed, our findings demonstrate the following: (1) The dominant hydrochemical facies are sodium-chloride (Na-Cl) near the coast, indicative of seawater intrusion, and calcium-bicarbonate (Ca-HCO_3) inland, reflecting water–rock interactions within the carbonate formations. The spatial distribution maps generated using IDW interpolation clearly delineate these facies and highlight areas exceeding WHO guidelines for chloride and nitrate. (2) The primary drivers of groundwater chemistry are both natural (carbonate mineral dissolution) and anthropogenic (agricultural practices, particularly fertilizer use and over-extraction leading to seawater intrusion). The PCA results underscore these influences, with component F1 reflecting mineralization and F2 highlighting saline intrusion. (3) The Témara Plain aquifer is highly vulnerable to seawater intrusion, particularly in the northern coastal areas where chloride concentrations exceed WHO guidelines, and agricultural contamination, evident in elevated nitrate levels in the southwestern agricultural zones exceeding WHO limits. These findings underscore the critical need for integrated and sustainable water resource management strategies in the Témara Plain. The observed water quality degradation, driven by the combined pressures of intensive agriculture, over-extraction, and seawater intrusion, poses significant risks to human health, agricultural productivity, and ecosystem integrity. The complex geological framework of the region further complicates these challenges, necessitating a nuanced and adaptive management approach. In this context, the development of a

detailed groundwater vulnerability map based on the DRASTIC model proves essential, as it provides a spatially explicit tool to identify high-risk zones and prioritize management efforts for the protection of the aquifer.

Author Contributions: Conceptualization, A.E.A., I.H., N.B., and B.M.; methodology, A.E.A., I.H., N.B., and B.M.; software, A.E.A., I.H., N.B., B.M., and Y.M.; validation, A.E.A., K.Y.F., S.M.A., E.R.A., B.M., and A.R.A.; formal analysis, M.A.H., K.Y.F., E.R.A., A.R.A., and S.M.A.; investigation, A.E.A., I.H., and B.M.; resources, A.E.A., I.H., and N.B.; data curation, A.E.A. and M.A.H.; writing—original draft preparation, A.E.A., I.H., N.B., B.M., and Y.M.; writing—review and editing, B.M., A.E.A., and M.A.H.; visualization, M.A.H., A.R.A., K.Y.F., S.M.A., and E.R.A.; project administration, M.A.H.; funding acquisition, K.Y.F. All authors have read and agreed to the published version of the manuscript.

Funding: This research was funded by Researchers Supporting Project number (PNURSP2025R673), Princess Nourah bint Abdulrahman University, Riyadh, Saudi Arabia.

Data Availability Statement: The data presented in this study are available on request from the corresponding author.

Acknowledgments: Princess Nourah bint Abdulrahman University Researchers Supporting Project number (PNURSP2025R673), Princess Nourah bint Abdulrahman University, Riyadh, Saudi Arabia.

Conflicts of Interest: The authors declare no conflicts of interest.

References

1. Jones, E.R.; Bierkens, M.F.P.; van Vliet, M.T.H. Current and Future Global Water Scarcity Intensifies When Accounting for Surface Water Quality. *Nat. Clim. Change* **2024**, *14*, 629–635. [CrossRef]
2. Kuang, X.; Liu, J.; Scanlon, B.R.; Jiao, J.J.; Jasechko, S.; Lancia, M.; Biskaborn, B.K.; Wada, Y.; Li, H.; Zeng, Z.; et al. The Changing Nature of Groundwater in the Global Water Cycle. *Science* **2024**, *383*, eadf0630. [CrossRef] [PubMed]
3. Wada, Y.; van Beek, L.P.H.; Bierkens, M.F.P. Modelling Global Water Stress of the Recent Past: On the Relative Importance of Trends in Water Demand and Climate Variability. *Hydrol. Earth Syst. Sci.* **2011**, *15*, 3785–3808. [CrossRef]
4. Das, A. Evaluation of Surface Water Quality in Brahmani River Basin, Odisha (India), for Drinking Purposes Using GIS-Based WQIs, Multivariate Statistical Techniques and Semi-Variogram Models. *Innov. Infrastruct. Solut.* **2024**, *9*, 484. [CrossRef]
5. Custodio, E.; Cabrera, M.C.; Sánchez-García, D.; de la Hera-Portillo, A.; García-Aróstegui, J.L.; Jódar, J.; Martos-Rosillo, S.; Puga, L.O.; Queralt, E. Proposal of Groundwater Governance Indexes: Application to Nine Spanish Aquifers. *Water Resour. Manag.* **2025**, *39*, 1–19. [CrossRef]
6. Khatita, A.M.A.; van Geldern, R.; Bamousa, A.O.; Alexakis, D.E.; Ismail, E.; Abdellah, W.R.; Babikir, I.A.A. Combining Hydro-Geochemistry and Environmental Isotope Methods to Evaluate Groundwater Quality and Health Risk (Middle Nile Delta, Egypt). *Hydrology* **2025**, *12*, 72. [CrossRef]
7. Tallini, M.; Adinolfi Falcone, R.; Carucci, V.; Falgiani, A.; Parisse, B.; Petitta, M. Isotope Hydrology and Geochemical Modeling: New Insights into the Recharge Processes and Water–Rock Interactions of a Fissured Carbonate Aquifer (Gran Sasso, Central Italy). *Environ. Earth Sci.* **2014**, *72*, 4957–4971. [CrossRef]
8. Liu, L.; Qi, S.; Wang, W. Groundwater Quality in Agricultural Lands Near a Rapidly Urbanized Area, South China. *Int. J. Environ. Res. Public Health* **2021**, *18*, 1783. [CrossRef]
9. Gómez-Navarro, O.; De Girolamo, A.M.; Lorenz, A.W.; Khadhar, S.; Debieche, T.-H.; Gentile, F.; Chiron, S.; Pérez, S. Characterization of Anthropogenic Impacts in Mediterranean Intermittent Rivers with Chemical, Ecological and Hydrological Indicators. *J. Hazard. Mater.* **2024**, *480*, 135951. [CrossRef]
10. Palatnik, R.R.; Raviv, O.; Sirota, J.; Shechter, M. Water Scarcity and Food Security in the Mediterranean Region: The Role of Alternative Water Sources and Controlled-Environment Agriculture. *Water Resour. Econ.* **2025**, *49*, 100256. [CrossRef]
11. Ceseracciu, C.; Nguyen, T.P.L.; Deriu, R.; Branca, G.; Vozinaki, A.-E.K.; Karatzas, G.P.; Mellah, T.; Akrout, H.; Yıldırım, Ü.; Kurt, M.A.; et al. Innovative Governance for Sustainable Management of Mediterranean Coastal Aquifers: Evidence from Sustain-COAST Living Labs. *Environ. Sci. Policy* **2025**, *167*, 104038. [CrossRef]
12. Fidelibus, M.D.; Balacco, G.; Alfio, M.R.; Arfaoui, M.; Bassukas, D.; Güler, C.; Hamzaoui-Azaza, F.; Külls, C.; Panagopoulos, A.; Parisi, A.; et al. A Chloride Threshold to Identify the Onset of Seawater/Saltwater Intrusion and a Novel Categorization of Groundwater in Coastal Aquifers. *J. Hydrol.* **2025**, *653*, 132775. [CrossRef]

13. Ibrahim, M.I.A.; El-Sawy, M.A.; Elgendy, A.R.; El-Sayed, H.M.; Mohamed, L.A.; Aly-Eldeen, M.A. Assessing Seawater Intrusion Impact on Groundwater Quality in El-Omayed Aquifers, Mediterranean Coast, Egypt Using Hydrogeochemical and Chemometric Analyses. *Groundw. Sustain. Dev.* **2025**, *29*, 101418. [CrossRef]
14. Ait Haddou, M.; Bouchriti, Y.; Ikirri, M.; Wanaim, A.; Aydda, A.; Amarir, S.; Amiha, R.; El Boudribili, Y. Delineation of Groundwater Potential Zones in a Semi-Arid Region Using Remote Sensing and GIS: A Case Study of Argana Corridor (Morocco). In *Advanced Technology for Smart Environment and Energy*; Mabrouki, J., Mourade, A., Irshad, A., Chaudhry, S.A., Eds.; Environmental Science and Engineering; Springer International Publishing: Cham, Switzerland, 2023; pp. 257–268. ISBN 978-3-031-25661-5. [CrossRef]
15. Görlich, I.; Weigand, S.; Beuel, S.; Bouchaou, L.; Reichert, B. Statusanalyse von Meerwasserintrusionen und Grundwasserhaushaltsmodellierung des oberen Küstenaquifers in Agadir, Marokko. *Grundwasser* **2015**, *20*, 25–37. [CrossRef]
16. Khattach, D.; El Gout, R.; Ziani, S.; Nouayti, A.; Nouayti, N.; Bouazza, M. Enhancing Subsurface Geological Imaging of Angad Basin (Northeastern Morocco) through the Integration of Gravity and Electrical Data: New Insights into the Jurassic Deep Aquifer for Groundwater Exploration and Development. *Geophys. J. Int.* **2025**, *241*, 1186–1203. [CrossRef]
17. Olías, M.; Basallote, M.D.; Cánovas, C.R.; Pérez-Carral, C. Groundwater Divide Shifting Due to Pumping in a Sector of the Doñana Aquifer System (SW Spain): Environmental Implications. *Environ. Monit. Assess.* **2025**, *197*, 526. [CrossRef]
18. Renau-Pruñonosa, A.; Esteller, M.V.; Aroba, J.; Grande, J.A.; Morell, I.; de la Torre, M.L.; García-Menéndez, O.; Ballesteros, B.J. Identification of Salinization Processes in Coastal Aquifers Using a Fuzzy Logic and Data Mining Based Methodology: Study Case in a Mediterranian Coastal Aquifer (Spain). *Environ. Earth Sci.* **2025**, *84*, 109. [CrossRef]
19. Benyoussef, S.; Arabi, M.; El Yousfi, Y.; Makkaoui, M.; Gueddari, H.; El Ouarghi, H.; Abdaoui, A.; Ghalit, M.; Zegzouti, Y.F.; Azirar, M.; et al. Assessment of Groundwater Quality Using Hydrochemical Process, GIS and Multivariate Statistical Analysis at Central Rif, North Morocco. *Environ. Earth Sci.* **2024**, *83*, 515. [CrossRef]
20. Zaland, R.A. Risk Assessment in Construction of Public Road Project in Afghanistan. *J. Achiev. Mater. Manuf. Eng.* **2022**, *110*, 70–85. [CrossRef]
21. Kmoch, L.; Bou-Lahriss, A.; Plieninger, T. Drought Threatens Agroforestry Landscapes and Dryland Livelihoods in a North African Hotspot of Environmental Change. *Landsc. Urban Plan.* **2024**, *245*, 105022. [CrossRef]
22. Richardson, C.M.; Davis, K.L.; Ruiz-González, C.; Guimond, J.A.; Michael, H.A.; Paldor, A.; Moosdorf, N.; Paytan, A. The Impacts of Climate Change on Coastal Groundwater. *Nat. Rev. Earth Environ.* **2024**, *5*, 100–119. [CrossRef]
23. Azemzi, H. Governance and Policy Approaches for Addressing Water Scarcity: Insights from Morocco. *Euro-Mediterr. J. Environ. Integr.* **2025**, *10*, 1–12. [CrossRef]
24. Boukhari, S.; Khalil, A.; Zouhri, L.; El Adnani, M. Geographic Information System-Based Database for Monitoring and Assessing Mining Impacts on Water Resources and Environmental Systems at National Scale: A Case Study of Morocco (North Africa). *Water* **2025**, *17*, 924. [CrossRef]
25. El Baroudi, H.; Ouazzani, C.; Moustaghfir, A.; Er-Ramly, A.; Essebbahi, I.; El Baroudi, Y.; Dami, A.; Balouch, L. Evaluation of Drinking Water Quality and Potential Health Risks on the Population in Morocco. *Desalination Water Treat.* **2024**, *320*, 100715. [CrossRef]
26. Nassri, I.; Harmouzi, H.; Tahri, L.; El Ouali, A.; Khattabi Rifi, S. Hydrogeochemical Assessment and Spatial Analysis of Groundwater Quality Parameters in North West of Morocco. *J. Saudi Soc. Agric. Sci.* **2024**, *23*. [CrossRef]
27. Elmotawakkil, A.; Sadiki, A.; Enneya, N. Predicting Groundwater Level Based on Remote Sensing and Machine Learning: A Case Study in the Rabat-Kénitra Region. *J. Hydroinformatics* **2024**, *26*, 2639–2667. [CrossRef]
28. Bahir, M.; El Mountassir, O.; Behnassi, M. Effect of Climate Change on Sea Water Intrusion in the Essaouira Basin Coastal Aquifer. In *The Water, Climate, and Food Nexus*; Springer: Cham, Switzerland, 2024; pp. 167–200, ISBN 978-3-031-50962-9. [CrossRef]
29. Karroum, M.; Elgettafi, M.; Elmandour, A.; Wilske, C.; Himi, M.; Casas, A. Geochemical Processes Controlling Groundwater Quality under Semi Arid Environment: A Case Study in Central Morocco. *Sci. Total Environ.* **2017**, *609*, 1140–1151. [CrossRef]
30. Qurtobi, M.; Hssaisoune, M.; Kumar, U.S.; Bouchaou, L. Multienvironmental Tracers in Coastal Aquifer (Morocco): A Window into Groundwater Mixing and Risk to Contamination. *Water Environ. Res.* **2024**, *96*, e10995. [CrossRef]
31. Zarati, A.; Zinedine, A.; Bakkali, F.; Rahim, S.; Bellali, F.; Bennani, M. Assessment of Groundwater Quality and Public Health Risks: Physicochemical and Bacteriological Analysis in the Casablanca-Settat Region, Morocco. *Int. J. Environ. Stud.* **2025**, *82*, 586–602. [CrossRef]
32. Kuriqi, A.; Abd-Elaty, I. Groundwater Salinization Risk in Coastal Regions Triggered by Earthquake-Induced Saltwater Intrusion. *Stoch. Environ. Res. Risk Assess.* **2024**, *38*, 3093–3108. [CrossRef]
33. Gonçalves, V.; Albuquerque, A.; Almeida, P.G.; Cavaleiro, V. DRASTIC Index GIS-Based Vulnerability Map for the Entre-Os-Rios Thermal Aquifer. *Water* **2022**, *14*, 2448. [CrossRef]
34. Zhang, J.; Peng, J.; Chen, X.; Shi, X.; Feng, Z.; Meng, Y.; Chen, W.; Liu, Y. Comparative Study on Different Interpolation Methods and Source Analysis of Soil Toxic Element Pollution in Cangxi County, Guangyuan City, China. *Sustainability* **2024**, *16*, 3545. [CrossRef]

35. Bivand, R.S.; Pebesma, E.; Gómez-Rubio, V. *Applied Spatial Data Analysis with R*; Springer: New York, NY, USA, 2013; ISBN 978-1-4614-7617-7.
36. Aman, H.; Doost, Z.H.; Hejran, A.W.; Mehr, A.D.; Szczepanek, R.; Gilja, G. Survey on The Challenges for Achieving SDG 6: Clean Water and Sanitation: A Global Insight. *Knowl.-Based Eng. Sci.* **2024**, *5*, 21–42. [CrossRef]
37. Mousazadeh, H. Unraveling the Nexus between Community Development and Sustainable Development Goals: A Comprehensive Mapping. *Community Dev.* **2025**, *56*, 276–302. [CrossRef]
38. Nandi, S.; Swain, S. Role of Groundwater Systems in Fulfilling Sustainable Development Goals: A Focus on SDG6 and SDG13. *Curr. Opin. Environ. Sci. Health* **2024**, *42*, 100576. [CrossRef]
39. Choubert, G.; El Azzouzi, M.; Boudad, M.; Lahouari, M. The Jurassic and Cretaceous of the Témara Region (Morocco): Stratigraphy and Paleogeography. *Rev. Paléobiologie* **1981**, 75–90.
40. Vidal, G.; Roussel, J.; Dupont, P.; Martin, L. *Carte Géologique de La Région de Romani à L'échelle 1:100,000*; Bureau de Recherches Géologiques et Minières: Paris, France, 1989.
41. Bucci, A.; Petrella, E.; Celico, F.; Naclerio, G. Use of Molecular Approaches in Hydrogeological Studies: The Case of Carbonate Aquifers in Southern Italy. *Hydrogeol. J.* **2017**, *25*, 1017–1031. [CrossRef]
42. Arabi, M.; Mechkirrou, L.; El Malki, M.; Alaoui, K.; Chaieb, A.; Maaroufi, F.; Karmich, S. Overview of Ecological Dynamics in Morocco—Biodiversity, Water Scarcity, Climate Change, Anthropogenic Pressures, and Energy Resources—Navigating Towards Ecosolutions and Sustainable Development. In Proceedings of the 4th Edition of Oriental Days for the Environment "Green Lab. Solution for Sustainable Development" (JOE4), Oujda, Morocco, 23–24 February 2024; In *E3S Web of Conferences Volume*. EDP Sciences: Paris, France, 2024; Volume 527, p. 01001. [CrossRef]
43. Schilling, J.; Freier, K.P.; Hertig, E.; Scheffran, J. Climate Change, Vulnerability and Adaptation in North Africa with Focus on Morocco. *Agric. Ecosyst. Environ.* **2012**, *156*, 12–26. [CrossRef]
44. Kalinin, V.V.; Kazak, A.V. Methods of Measuring Electric Conductivity of Surface Natural Water: Experimental Results. *Moscow Univ. Geol. Bull.* **2008**, *63*, 178–184. [CrossRef]
45. World Health Organization. *Guidelines for Drinking-Water Quality [Electronic Resource]: Incorporating 1st and 2nd Addenda, Vol.1, Recommendations*, 3rd ed.; World Health Organization: Geneva, Switzerland, 2008; ISBN 978-92-4-154761-1.
46. Wilcox, L.V. *Classification and Use of Irrigation Waters*; Forgotten Books: London, UK, 2018.
47. Appelo, C.A.J.; Postma, D. *Geochemistry, Groundwater and Pollution*, 2nd ed.; CRC Press: Boca Raton, FL, USA, 2010; ISBN 978-0-415-36421-8.
48. Drever, J.I. *The Geochemistry of Natural Waters*, 2nd ed.; Prentice Hall: Englewood Cliffs, NJ, USA, 1988; ISBN 978-0-13-351396-7.
49. Hounslow, A.W. *Water Quality Data: Analysis and Interpretation*, 1st ed.; Taylor & Francis Group: Bosa Roca, FL, USA, 1995; ISBN 978-0-87371-676-5.
50. Hem, J.D. *Study and Interpretation of the Chemical Characteristics of Natural Water*; U.S. Department of the Interior: Washington, DC, USA, 1959.
51. Alemu, C.M.; Aycheh, Y.F.; Angualie, G.S.; Engidayehu, S.S. Modeling on Comprehensive Evaluation of Groundwater Quality Status Using Geographic Information System (GIS) and Water Quality Index (WQI): A Case Study of Bahir Dar City, Amhara, Ethiopia. *Water Pract. Technol.* **2024**, *19*, 1084–1098. [CrossRef]
52. Caloiero, T.; Pellicone, G.; Modica, G.; Guagliardi, I. Comparative Analysis of Different Spatial Interpolation Methods Applied to Monthly Rainfall as Support for Landscape Management. *Appl. Sci.* **2021**, *11*, 9566. [CrossRef]
53. Liu, D.; Zhao, Q.; Fu, D.; Guo, S.; Liu, P.; Zeng, Y. Comparison of Spatial Interpolation Methods for the Estimation of Precipitation Patterns at Different Time Scales to Improve the Accuracy of Discharge Simulations. *Hydrol. Res.* **2020**, *51*, 583–601. [CrossRef]
54. Scavia, D.; Field, J.C.; Boesch, D.F.; Buddemeier, R.W.; Burkett, V.; Cayan, D.R.; Fogarty, M.; Harwell, M.A.; Howarth, R.W.; Mason, C.; et al. Climate Change Impacts on U.S. Coastal and Marine Ecosystems. *Estuaries* **2002**, *25*, 149–164. [CrossRef]
55. Igaz, D.; Šinka, K.; Varga, P.; Vrbičanová, G.; Aydın, E.; Tárník, A. The Evaluation of the Accuracy of Interpolation Methods in Crafting Maps of Physical and Hydro-Physical Soil Properties. *Water* **2021**, *13*, 212. [CrossRef]
56. Tan, Q.; Xu, X. Comparative Analysis of Spatial Interpolation Methods: An Experimental Study. *Sens. Transducers* **2014**, *165*, 155–163.
57. Wang, H.; Cao, H.; Yang, L. Machine Learning-Driven Multidomain Nanomaterial Design: From Bibliometric Analysis to Applications. *ACS Appl. Nano Mater.* **2024**, *7*, 26579–26600. [CrossRef]
58. Yang, L.; Wang, H.; Leng, D.; Fang, S.; Yang, Y.; Du, Y. Machine Learning Applications in Nanomaterials: Recent Advances and Future Perspectives. *Chem. Eng. J.* **2024**, *500*, 156687. [CrossRef]
59. Grace N, V.A.; Aldehim, G.; Alruwais, N.; T.N., P. Novel PCA-Driven Extreme Machine Learning for Comprehensive Modelling of Metropolitan Wastewater Treatment Systems. *Desalination Water Treat.* **2025**, *321*, 101037. [CrossRef]
60. Xie, Z.; Liu, W.; Chen, S.; Yao, R.; Yang, C.; Zhang, X.; Li, J.; Wang, Y.; Zhang, Y. Machine Learning Approaches to Identify Hydrochemical Processes and Predict Drinking Water Quality for Groundwater Environment in a Metropolis. *J. Hydrol. Reg. Stud.* **2025**, *58*, 102227. [CrossRef]

61. Goodarzi, M.R.; Bafrouei, H.B.; Vazirian, M. Insight into Groundwater Level Prediction with Feature Effectiveness: Comparison of Machine Learning and Numerical Methods. *Hydrol. Res.* **2024**, *56*, 74–92. [CrossRef]
62. Albuquerque, A.; Scalize, P.S.; Ferreira, N.C.; Silva, F. Multi-Criteria Analysis for Site Selection for the Reuse of Reclaimed Water and Biosolids. *Rev. Ambient. Água* **2015**, *10*, 22–34. [CrossRef]
63. Teixeira, J.; Chaminé, H.I.; Carvalho, J.M.; Pérez-Alberti, A.; Rocha, F. Hydrogeomorphological Mapping as a Tool in Groundwater Exploration. *J. Maps* **2013**, *9*, 263–273. [CrossRef]
64. Aller, L.; Lehr, J.H.; Petty, R.; Bennett, T. DRASTIC: A Standardized System to Evaluate Groundwater Pollution Potential Using Hydrogeologic Setting. *J. Geol. Soc. India* **1987**, *29*, 23–37. [CrossRef]
65. Al-Zabet, T. Evaluation of Aquifer Vulnerability to Contamination Potential Using the DRASTIC Method. *Env. Geol.* **2002**, *43*, 203–208. [CrossRef]
66. Wei, X.; Zhou, Y.; Ran, L.; Chen, M.; Zou, J.; Fan, Z.; Fu, Y. Sources and Transformation of Nitrate in Shallow Groundwater in the Three Gorges Reservoir Area: Hydrogeochemistry and Isotopes. *Water* **2024**, *16*, 3299. [CrossRef]
67. Al-Aizari, H.S.; Aslaou, F.; Al-Aizari, A.R.; Al-Odayni, A.-B.; Al-Aizari, A.-J.M. Evaluation of Groundwater Quality and Contamination Using the Groundwater Pollution Index (GPI), Nitrate Pollution Index (NPI), and GIS. *Water* **2023**, *15*, 3701. [CrossRef]
68. Zaryab, A.; Farahmand, A.; Jafari, Z.; Ali, S.; Alijani, F.; Nassery, H.R. Geochemical Evolution of Spring Waters in Carbonate Dominated Aquifer in Upper Shirin Tagab Sub-Basin, Northern Afghanistan. *Groundw. Sustain. Dev.* **2024**, *25*, 101102. [CrossRef]
69. Qiu, Y.; Zhou, A.; Gao, L.; Wang, Z.; Hu, X.; Li, Y.; Zhang, F.; Ma, C. Cation Exchange and Leakage as Dominant Processes in Controlling Salinity and Strontium in Sandy and Argillaceous Coastal Aquifer: Insights from Hydrochemistry and Multi-Isotopes. *J. Hydrol.* **2024**, *638*, 131529. [CrossRef]
70. Boualem, B.; Egbueri, J.C. Graphical, Statistical and Index-Based Techniques Integrated for Identifying the Hydrochemical Fingerprints and Groundwater Quality of In Salah, Algerian Sahara. *Environ. Geochem. Health* **2024**, *46*, 158. [CrossRef]
71. Liu, N.; Chen, M.; Gao, D.; Wu, Y.; Wang, X. Identification of Hydrogeochemical Processes in Shallow Groundwater Using Multivariate Statistical Analysis and Inverse Geochemical Modeling. *Environ. Monit. Assess.* **2025**, *197*, 135. [CrossRef]
72. Zheng, H.; Mao, X.; Peng, H.; Cai, W.; Yuan, Y.; Zha, X.; Zhao, Z.; Liu, J. The Impacts of Evaporites on the Hydrogeochemical Processes of Brackish Groundwater in the Huangshui River Basin, Northwest China. *Hydrol. Process.* **2024**, *38*, e70041. [CrossRef]
73. Wijerathne, D.; Samarasekara, R.S.M.; Satanarachchi, N.; Vithanage, M.; Lakmal, H.M.A. Evaluating the Environmental Impacts of Hard Coastal Engineering Structures on Groundwater Salinity and Salinity Intrusion: Insights from the Marawila Coastal Zone, Sri Lanka. *Environ. Chall.* **2025**, *19*, 101145. [CrossRef]
74. Ait Lemkademe, A.; El Ghorfi, M.; Zouhri, L.; Heddoun, O.; Khalil, A.; Maacha, L. Origin and Salinization Processes of Groundwater in the Semi-Arid Area of Zagora Graben, Southeast Morocco. *Water* **2023**, *15*, 2172. [CrossRef]
75. El Mountassir, O.; Bahir, M. The Assessment of the Groundwater Quality in the Coastal Aquifers of the Essaouira Basin, Southwestern Morocco, Using Hydrogeochemistry and Isotopic Signatures. *Water* **2023**, *15*, 1769. [CrossRef]
76. Rivett, M.O.; Budimir, L.; Mannix, N.; Miller, A.V.M.; Addison, M.J.; Moyo, P.; Wanangwa, G.J.; Phiri, O.L.; Songola, C.E.; Nhlema, M.; et al. Responding to Salinity in a Rural African Alluvial Valley Aquifer System: To Boldly Go beyond the World of Hand-Pumped Groundwater Supply? *Sci. Total Environ.* **2019**, *653*, 1005–1024. [CrossRef] [PubMed]
77. Mastrocicco, M.; Colombani, N. The Issue of Groundwater Salinization in Coastal Areas of the Mediterranean Region: A Review. *Water* **2021**, *13*, 90. [CrossRef]
78. Verruijt, A. A Note on the Ghyben-Herzberg Formula. *Int. Assoc. Sci. Hydrology. Bull.* **1968**, *13*, 43–46. [CrossRef]
79. Su, Q.; Kambale, R.D.; Tzeng, J.-H.; Amy, G.L.; Ladner, D.A.; Karthikeyan, R. The Growing Trend of Saltwater Intrusion and Its Impact on Coastal Agriculture: Challenges and Opportunities. *Sci. Total Environ.* **2025**, *966*, 178701. [CrossRef]
80. Cherkaoui, T.-E.; El Hassani, A. Seismicity and Seismic Hazard in Morocco. *Bull. L'institut Sci.* **2012**, *34*, 45–55.
81. Argamasilla, M.; Barberá, J.A.; Andreo, B. Factors Controlling Groundwater Salinization and Hydrogeochemical Processes in Coastal Aquifers from Southern Spain. *Sci. Total Environ.* **2017**, *580*, 50–68. [CrossRef]
82. Ziani, D.; Boudoukha, A.; Boumazbeur, A.; Benaabidate, L.; Fehdi, C. Investigation of Groundwater Hydrochemical Characteristics Using the Multivariate Statistical Analysis in Ain Djacer Area, Eastern Algeria. *Desalination Water Treat.* **2016**, *57*, 26993–27002. [CrossRef]
83. Moussaoui, Z.; Gentilucci, M.; Wederni, K.; Hidouri, N.; Hamedi, M.; Dhaoui, Z.; Hamed, Y. Hydrogeochemical and Stable Isotope Data of the Groundwater of a Multi-Aquifer System in the Maknessy Basin (Mediterranean Area, Central Tunisia). *Hydrology* **2023**, *10*, 32. [CrossRef]
84. Bahir, M.; Ouazar, D.; Ouhamdouch, S. Hydrogeochemical Investigation and Groundwater Quality in Essaouira Region, Morocco. *Mar. Freshw. Res.* **2019**, *70*, 1317–1332. [CrossRef]
85. Bahir, M.; Carreira, P.; Oliveira Da Silva, M.; Fernandes, P. Caractérisation Hydrodynamique, Hydrochimique et Isotopique Du Système Aquifère de Kourimat (Bassin d'Essaouira, Maroc). *Estud. Geol.* **2008**, *64*, 61–73. [CrossRef]

86. McGrane, S.J. Impacts of Urbanisation on Hydrological and Water Quality Dynamics, and Urban Water Management: A Review. *Hydrol. Sci. J.* **2016**, *61*, 2295–2311. [CrossRef]
87. UN-Water. *World Water Development Report*; UN-Water: New York, NY, USA, 2020.
88. Foster, S.S.D.; Chilton, P.J. Groundwater: The Processes and Global Significance of Aquifer Degradation. *Phil. Trans. R. Soc. Lond. B* **2003**, *358*, 1957–1972. [CrossRef] [PubMed]
89. Gouahi, S.; Hssaisoune, M.; Qurtobi, M.; Nehmadou, M.; Bouaakaz, B.; Boudhair, H.; Bouchaou, L. Managed Aquifer Recharge in a Semi-Arid Basin: A Case Study from the Souss Aquifer, Morocco. In *Managed Groundwater Recharge and Rainwater Harvesting*; Saha, D., Villholth, K.G., Shamrukh, M., Eds.; Water Resources Development and Management; Springer Nature: Singapore, 2024; pp. 129–150, ISBN 978-981-99-8756-6.
90. Plan National 2020-2050. Morocco.
91. Margat, J.; van der Gun, J. *Groundwater Around the World: A Geographic Synopsis*; CRC Press: Boca Raton, FL, USA, 2013; ISBN 978-1-138-00034-6.
92. Gleeson, T.; Wada, Y.; Bierkens, M.F.P.; Van Beek, L.P.H. Water Balance of Global Aquifers Revealed by Groundwater Footprint. *Nature* **2012**, *488*, 197–200. [CrossRef]
93. Basraoui, N.; Ben-Tahar, R.; Basraoui, Y.; EL Guerrouj, B.; Chafi, A. Water Quality Assessment in the Moulouya Estuary (Northeastern Morocco): The Effect of Wastewater on Microbiological and Physicochemical Properties. *Reg. Stud. Mar. Sci.* **2024**, *78*, 103736. [CrossRef]
94. Scanlon, B.R.; Reedy, R.C.; Stonestrom, D.A.; Prudic, D.E.; Dennehy, K.F. Impact of Land Use and Land Cover Change on Groundwater Recharge and Quality in the Southwestern US. *Glob. Change Biol.* **2005**, *11*, 1577–1593. [CrossRef]